INSTITUTO SUPERIOR DE ENGENHARIA DE LISBOA

Departamento de Engenharia de Electrónica e Telecomunicações e de Computadores

Antenas para aplicações biomédicas

André Miguel de Jesus Almeida Ribeiro

Dissertação para obtenção do Grau de Mestre
em Engenharia Eletrónica e Telecomunicações

Orientadores : Doutor Carlos Alberto Barreiro Mendes
Doutor Pedro Renato Tavares Pinho

Júri:

Presidente: Doutora Paula Maria Garcia Louro

Vogais: Doutor Daniel Filipe Albuquerque
Doutor Carlos Alberto Barreiro Mendes

JUNHO, 2024

INSTITUTO SUPERIOR DE ENGENHARIA DE LISBOA

Departamento de Engenharia de Electrónica e Telecomunicações e de Computadores

Antenas para aplicações biomédicas

André Miguel de Jesus Almeida Ribeiro

Dissertação para obtenção do Grau de Mestre
em Engenharia Eletrónica e Telecomunicações

Orientadores : Doutor Carlos Alberto Barreiro Mendes
Doutor Pedro Renato Tavares Pinho

Júri:

Presidente: Doutora Paula Maria Garcia Louro

Vogais: Doutor Daniel Filipe Albuquerque
Doutor Carlos Alberto Barreiro Mendes

JUNHO, 2024

À minha namorada

Acknowledgments

First of all, I would like to thank my supervisors, Professor Carlos Alberto Barreiro Mendes and Professor Pedro Renato Tavares Pinho, for all the patience and assistance they provided me during this project. The advices given in CST and during the measurement of the antennas were crucial to the development of this thesis. I would also like to thank ISEL and Universidade de Aveiro for providing the materials and the means to fabricate and measure the antennas performance. I would also like to thank my parents for all the support throughout my academic and personal journey and finally, I would like to thank all my course colleagues and friends who have helped me over the years at ISEL and provided great memories.

Abstract

Electromagnetic signals have been used in healthcare making possible many noninvasive techniques for diagnosis and treatment. Antennas play a key role in transmitting waves, requiring strong design for effective medical devices.

Supported by the appealing use of non-ionizing radiation, this dissertation presents a study on the design, manufacturing and measurement of in-body and on-body antennas for the 2.45 GHz ISM frequency band.

Two slightly different versions of a new in-body antenna were designed. A detailed description of the procedure followed to achieve a compact antenna is presented. Dimensions of the antennas are 13 x 13 x 3.2 mm and 19 x 19 x 3.2 mm. Glue was used in order to hold the superstrate in the smaller antenna, while screws were used to hold the superstrate in the bigger antenna. For the on-body antenna a previously designed antenna by the author of this dissertation will be used.

Transmission between antennas showed positive results with a transmission coefficient of -75 dB at 2.45 GHz. Additionally, transmission between antennas improved significantly when the in-body antenna was positioned at the center of the phantom, with a transmission value of -40 dB.

Experimental results (namely input impedance matching) are used to validate the theoretical design. A good similarity between theory and measurement is achieved, thus validating the design procedure.

SAR values for all antennas were also calculated and used to determine the maximum allowed input power to the antennas. Finally, a link-budget analysis between in-body and on-body antennas is presented. When the antenna was placed at the center of the phantom, throughput values reached 97 and 107 Gb/s for the in-body glue antenna and the in-body screws antenna, respectively.

Keywords: ISM, In-body antennas, On-body antennas, SAR, Numerical phantom, Body-centric link budget, compact printed antennas, antenna measurements;

Resumo

A radiação eletromagnética tem sido utilizada de diversas formas na área da saúde nos últimos anos. O uso de ondas eletromagnéticas tem possibilitado muitos métodos não invasivos de diagnóstico e tratamento de doenças. As antenas são responsáveis por transmitir e receber ondas eletromagnéticas, levando a que um bom design destas seja crucial para dimensionar dispositivos que possam ajudar médicos e pacientes.

Baseado nas vantagens do uso de radiação não-ionizante, esta dissertação apresenta um estudo sobre o design e a construção de antenas *in-body* e *on-body* para a faixa de frequência ISM 2.45 GHz.

Duas versões de antenas *in-body* foram desenhadas. Uma descrição detalhada do processo de miniaturização da antena é apresentado. A antena mais pequena tem 13 x 13 x 3.2 mm de dimensões e a maior tem 19 x 19 x 3.2 mm. A grande diferença entre estas duas antenas é a fixação do superstrato; numa o superstrato é fixo com cola, na outra é fixo com parafusos. As antenas cobrem toda a faixa de frequência ISM 2.45 GHz. Para a antena *on-body* foi utilizada uma antena microstrip alimentada por fenda.

A transmissão entre antenas apresentou bons resultados com o valor do coeficiente de transmissão a -75 dB. Quando a antena é colocada no centro do phantom, o valor de coeficiente de transmissão melhora para -40 dB.

Os resultados experimentais são utilizados para validar a proposta teórica da antena. Os resultados experimentais e teóricos obtidos são semelhantes, validando o processo de desenho da antena.

Os valores de SAR também são calculados e utilizados para determinar a potência de alimentação máxima das antennas. Foi também feito um estudo do *link budget* entre as antenas *in-body* e a antena *on-body*. Dependendo da BER e da posição das antenas dentro do phantoma, é possível atingir débitos entre 97 e 107 Gb/s.

Palavras-chave: ISM, Antenas *in-body*, Antenas *on-body*, SAR, phantoma, *link-budget*, antenas miniaturizadas, medições de antenas;

Contents

List of Figures

List of Tables

Acronyms

BER Bit error rate. 58, 59

CPW Coplanar Waveguide. 8
CST Computer Simulation Technology. 5

FCC Federal Communications Commission. 2, 4

GI GastroIntestinal. 1, 12

IMD Implantable Medical Devices. 1
ISM Industrial Scientific and Medical. 2, 8, 9, 10, 11, 12, 13, 14, 15, 28, 29, 40, 46, 49, 52, 67, 68

MICS Medical Implant Communications Service. 2, 7, 8, 9, 10, 12, 13

PIFA Planar Inverted-F Antenna. 8, 10

SAR Specific Absorption Rate. 4, 53, 57, 68

UWB UltraWide Band. 2

VNA Vector Network Analyzer. 61

WCE Wireless Capsule Endoscopy. 1

WMTS Wireless Medical Telemetry Services. 2, 8, 12, 14

ZOR Zeroth-order resonance. 10

1

Introduction

1.1 Applications in healthcare field

Electromagnetic signals have been used in a variety of ways in the healthcare field over the last few years. The use of electromagnetic waves has made possible many noninvasive methods of diagnosis and treatment of illnesses. Antennas are responsible for transmitting and receiving electromagnetic waves therefore a good design is crucial in order to build devices that can help doctors and patients alike.

Antennas are used in a wide range in medical applications as shown in figure 1.1. The antenna may be fixed inside the human body (pacemaker, monitoring of diabetes, Increased Intracranial Pressure monitoring devices) or travel through the human body (Wireless Capsule Endoscopy (WCE)). The former are called Implantable Medical Devices (IMD) [1].

For WCE's the patient swallows a small capsule with an embedded camera. Because of the limited available size, antennas wrapped or printed on the outer wall of the capsule are advantageous, saving the inner volume of the capsule for other electronic components. The GastroIntestinal (GI) tract is composed by various tissues, all with different permittivity values. The antenna must have sufficient bandwidth in order to accommodate frequency detuning caused by the various tissues present in the GI tract. Wide bandwidth is also necessary for the transmission of high-resolution images that are required for the imaging of the GI tract [1].

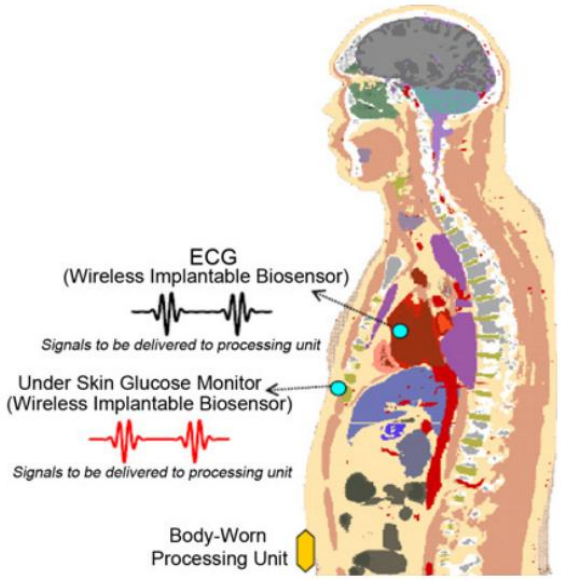

Figure 1.1: Applications of implantable antennas (taken from [1])

Regulators have approved several bands of frequency for medical use. The Medical Implant Communications Service (MICS) covers the 402-405 MHz frequency range and is used for implant communications. There is also the Wireless Medical Telemetry Services (WMTS) frequency band. This frequency band covers the 608–614 MHz, 1395–1400 MHz, 1427–1432 MHz frequencies and is designed by the Federal Communications Commission (FCC) for remote health monitoring of patients [2]. This band provides an interference-free spectrum preventing overcrowding present in more popular bands. The Industrial Scientific and Medical (ISM) frequency band is available worldwide and supports high data rate applications (2400-2483.5MHz). Finally there is the UltraWide Band (UWB), covering the 3.1-10.76 GHz frequency range. UWB systems have been considered as a potential candidate for future in-body devices due to large bandwidth and low power consumption. Despite that, the attenuation through the biological tissues increases dramatically as the frequency increases. For example, at frequencies between 3 and 5 GHz attenuation is as high as 20-30 dB for every 2 cm of biological tissue [3].

Until a revision of standards happens however, the antenna engineer must respect the IEEE 802.15.6 standard, which was released by the IEEE in 2012 to deal with short-range, wireless communications in the vicinity of, or inside, the human body. According to the standard, a wireless device shall be able to support transmission and reception in at least one of the following frequency bands: 402–405, 420–450, 863–870, 902–928, 950–958, 2360–2400, and 2400–2483.5 MHz [4].

All bands are shown in figure 1.2.

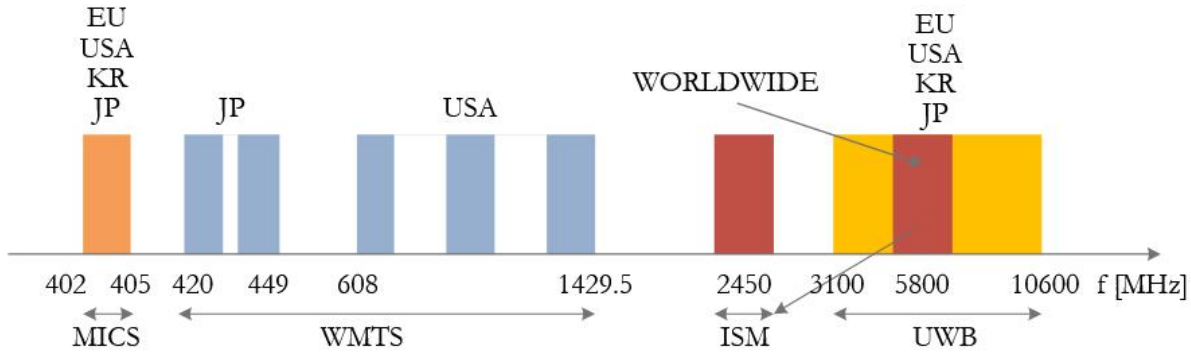

Figure 1.2: Frequency bands regulated by regulators worldwide (taken from [5])

1.2 Antenna design challenges

The antenna engineer must have a few characteristics in mind while designing the antenna such as radiation efficiency, dimensions, bandwidth and frequency of operation. Human body proximity also provides a challenge to the antenna engineer, who must take into account the potential for coupling caused by it resulting in a significant reduction of power, frequency shifts and radiation pattern distortion. While at lower frequencies the design of the antenna faces fewer challenges, they are limited to lower communication speeds (1-30kbps) making their use not ideal [6] [7].

There are three types of scenarios to consider when designing antennas with the human body nearby: [8]

- For off-body scenarios the propagation direction points away from the human body;
- For on-body scenarios the propagation path is defined alongside the body surface and the antenna is located in close proximity of the body;
- For in-body scenarios the main propagation path leads through the tissue of the human body.

Off-body scenarios generally require no modifications of the far field model in order to estimate antenna performance. However both in-body and on-body scenarios require changes to the propagation models. In [8] researchers study those modifications. They were able to develop new propagation models that estimate directivity and effective antenna area for these scenarios.

The devices must be as unobtrusive as possible. The engineer has to design the antenna in order to be as compact and lightweight any way they can. The compression of

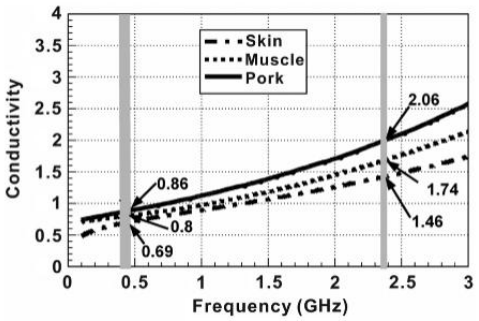

(a) Conductivity of pork, muscle and skin

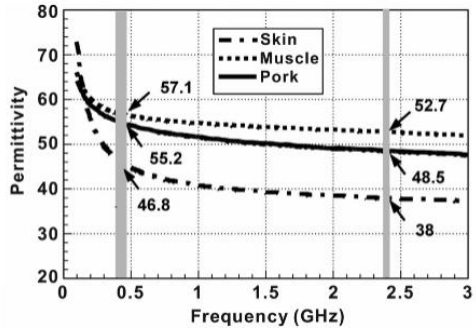

(b) Permittivity of pork, muscle and skin

Figure 1.3: Conductivity and permittivity of pork, muscle and skin (taken from [11])

the antenna will affect the bandwidth and efficiency thus adding challenges to the difficulties already present by the proximity of the human body. Antenna type is also key to achieve a good performance despite the challenges. As an example adding a ground plane between the antenna and the body will reduce the effects of the latter on the former. Depending on the scenario radiation pattern is also important [5].

Absorption of radiation by the human tissue needs to be considered. This is characterized by the maximum allowed Specific Absorption Rate (SAR). According to the FCC SAR values cannot be greater than 1.6 W/kg, averaged over 1g of tissue and no greater than 2 W/kg, averaged of 10g of tissue [5].

Another problem present in this type of applications is the biocompatibility of the antenna. There are two options in order to design an antenna biocompatible with the human body; using biocompatible materials in the antenna itself, or adding a biocompatible layer to encapsulate a conventional antenna. For the former, researchers have found that using biocompatible materials doesn't affect the performance of the antenna, which was expected since the dielectric properties are similar [9]. In [10] researchers study the effect of adding a biocompatible layer to a conventional antenna. They found that the biocompatible layer can improve the radiation efficiency by up to six times. This is explained by the facilitation of the electromagnetic transition from the biological tissue to free-space.

To measure antenna performance accurately the material used in testing must resemble the electric properties of the human body. Minced pork can be used in order to provide a simple and easy approach to mimic the human body and validate antenna performance. In figure 1.3 the conductivity and permittivity of pork are shown and compared with skin and muscle properties. Between 100 MHz and 3 GHz pork tissue is similar to muscle providing a good material to measure antenna performance [11].

1.3 Objectives

The goals of the thesis are:

1. Design an in-body antenna for the ISM 2.45 GHz frequency band;
2. Study miniaturization techniques in order to compact the antenna for in-body use;
3. Test the performance of the antennas inside pork tissue and validate results;
4. Study the transmission between the in-body antenna and an on-body antenna.

Computer Simulation Technology (CST) Microwave Studio is going to be used in order to simulate antenna performance in free-space and inside the human body.

1.4 Contributions originated by this thesis

This thesis resulted in this contributions:

1. **A. Ribeiro, C. Mendes, P. Pinho**, "Transmission study between in-body and on-body antennas in the ISM 2.45 GHz frequency band", for the XV Iberian Meeting on Computational Electromagnetics, November 14th-17th 2023, Cádiz, Spain - **Published**
2. **A. Ribeiro, C. Mendes, P. Pinho**, "In-body and on-body antennas for the ISM 2.45 GHz band", for ICEEA - IEEE APWC, September 2-6, 2024, Lisbon, Portugal - **Accepted for oral presentation**

2

State of the art

There has been a lot of research in regards to designing and manufacturing antennas for the three scenarios mentioned in chapter 1. This chapter will focus on antennas for in-body applications.

Antennas for in-body applications can be split in two categories based on the way of insertion into the human body [3]:

- Implantable antennas;
- Ingestible antennas;

This chapter will focus on these categories.

2.1 Implantable antennas

Implantable antennas are placed inside the human body usually by means of surgery. Since implantable antennas are fixed inside the human body, they must be biocompatible in order to preserve patient safety and rejection of the implant. The most widely used materials to encapsulate the implantable antenna are Teflon, Alumina Ceramic and Macor [1]. These antennas usually operate in the MICS (402 MHz-405 MHz) and ISM 2.45 GHz frequency bands.

In [12] a Coplanar Waveguide (CPW) fed monopole was designed for the 2.45 GHz ISM band (Figure 2.1). Ceramic alumina was used as substrate due to its biocompatibility with the human body. The antenna, which was measured surrounded by pork tissue, achieved a return loss of -27.8 dB and has a 220 MHz bandwidth that covers the entire 2.45 GHz ISM band.

Figure 2.1: Implantable CPW fed monopole for 2.45 GHz ISM band (taken from [12])

In [13] researchers propose an antenna for a retinal prosthesis system operating in the MICS (402 MHz-405 MHz) frequency band. Researcher were able to achieve a fairly small antenna with 12 x 12 x 1.9 mm in dimensions. With a return loss peak of -12.42 dB the antenna has a decent performance despite the high dielectric constant of the eye (ε_r = 69 at 402MHz). This antenna however is based on simulated results and requires validation with actual measurements.

In [14] researchers propose a Planar Inverted-F Antenna (PIFA) based antenna with a slot in order to compact it (figure 2.2). Antenna dimensions measure 19 x 30 x 1.6 mm. This antenna covers three frequency bands (MICS, WMTS and ISM) and is compacted with the use of a shorting pin. According to the authors this antenna is suitable for implanting in the arm or under the chest.

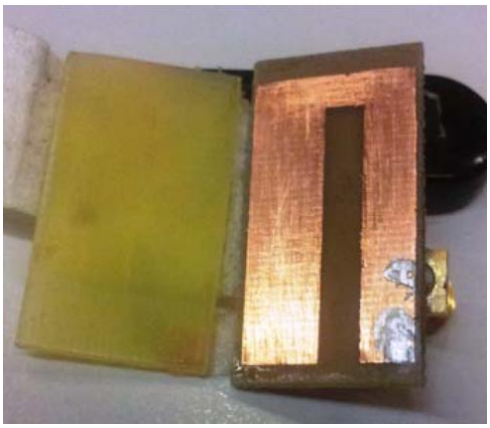

Figure 2.2: PIFA based triple band antenna (taken from [14])

In [11] a spiral antenna was suggested. The antenna has compact size of 10 x 10 x 2.54 mm. It consists of three layers of substrate connected via shorting pins and one layer of superstrate. The antenna has a bandwidth of 86 MHz for the MICS band and 60 MHz for the ISM band, not covering it completely. In figure 2.3 the layers are shown. The use of the shorting pins and slits turn this antenna into a very compact device.

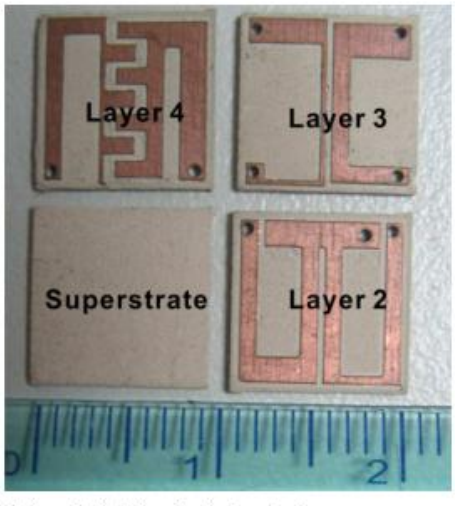

Figure 2.3: Spiral antenna for MICS and ISM frequency bands (taken from [11])

In [15] a patch antenna was proposed. The antenna is fairly small with a size of 7 x 7 x 0.254 mm and is presented in figure 2.4. The small size is due to the shorting pin and a bear shaped slit on patch and slits in the ground plane. The antenna covers the ISM 915 MHz frequency band with a bandwidth of 220 MHz.

Figure 2.4: Bear shaped microstrip antenna for the 915 MHz ISM frequency band (taken from [15])

In [16] a four-layered compact PIFA antenna is designed. Antenna dimensions are 3.14 x 7.5 x 2.54 mm and it covers the MICS frequency band. The antena is compact due to the use of a high permittivity material as substrate. The stacked PIFA structure increases the length of the current flow path allowing the antenna to be miniaturized.

In [17] a compact implantable Zeroth-order resonance (ZOR) antenna is proposed. This antenna measures 15.9 x 12.9 x 1.6 mm and its dimensions are possible due to the use of chip inductors. This antenna has 9 MHz of bandwidth and operates in the MICS band. This antenna is shown in figure 2.5.

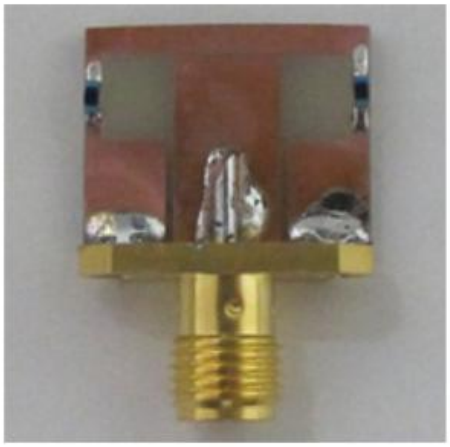

Figure 2.5: Compact zeroth-order resonance antenna operating in the MICS frequemcy band (taken from [17])

In [18] a miniaturized dual-band implantable antenna using meandered line resonator is proposed. This antenna covers two ISM frequency bands (0.91 GHz and 2.45 GHz). The antenna is miniaturized using meandered resonators and slots inserted in the

ground plane. The antenna is inserted inside a capsule which helps decrease the coupling caused by the phantom.

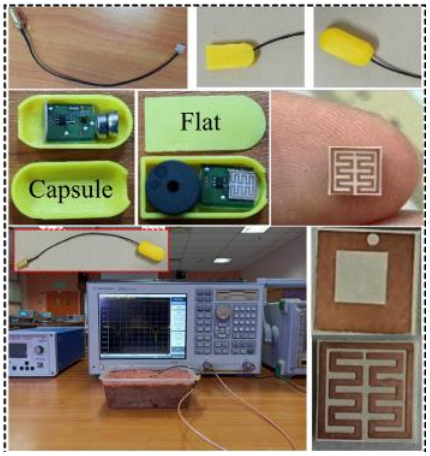

Figure 2.6: Compact zeroth-order resonance antenna operating in the MICS frequency band (taken from [18])

In [19] a compact implantable antenna for the ISM 2.45 GHz frequency band is designed (figure 2.7). The size of the antenna is miniaturized due the use of a high permittivity material as substrate and a folded meander structure. The antenna measures 3 x 3 x 0.5 mm and covers the whole ISM 2.45 GHz frequency band.

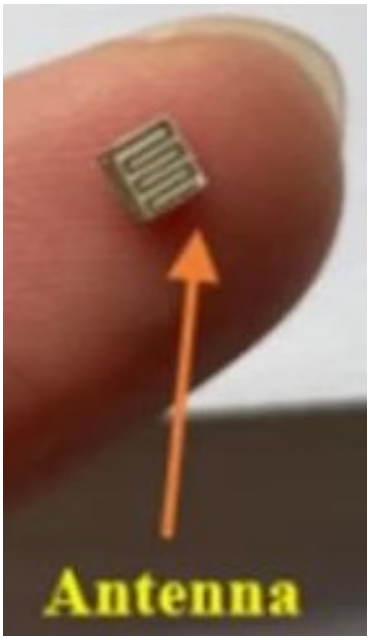

Figure 2.7: Folded meander antenna the 2.45 GHz ISM frequency band (taken from[19])

In table 2.1 a collection of some implatable antennas are presented.

Table 2.1: Implantable antennas present in literature

Implantable Antennas				
Antenna Type	*Bandwidth (MHz)*	*Size (mm)*	*Frequency band*	*Citation*
Monopole	220	10 x 14 x 0.65	ISM	[12]
PIFA	39	12 x 12 x 1.9	MICS	[13]
PIFA	16 100 200	19 x 30 x 1.6	MICS WMTS ISM	[14]
Spiral	113 70	10 x 10 x 2.54	MICS ISM	[11]
Patch	220	7 x 7 x 0.254	ISM	[15]
PIFA	50	3.14 x 7.5 x 2.54	MICS	[16]
ZOR	9	15.9 x 12.9 x 1.6	MICS	[17]
Meandered	94 160	5.6 x 5.8 x 0.25	ISM	[18]
Patch	150	3 x 3 x 0.5	ISM	[19]

2.2 Ingestible antennas

Ingestible antennas are antennas that travel through the GI track and diagnose GI related cancers. These have been important in recent years due to getting to parts of the GI previously unreachable by Gastroscopy and Colonoscopy [1]. These antennas operate in MICS, WMTS and ISM 2.45 GHz frequency bands.

In [20] a spiral antenna is suggested for the MICS frequency band. It has a bandwidth of 70 MHz and a size of 10.1 x 10.1 mm as shown in figure 2.8. The spiral shape of the antenna forms a longer current path flow, allowing for the miniaturization of the antenna.

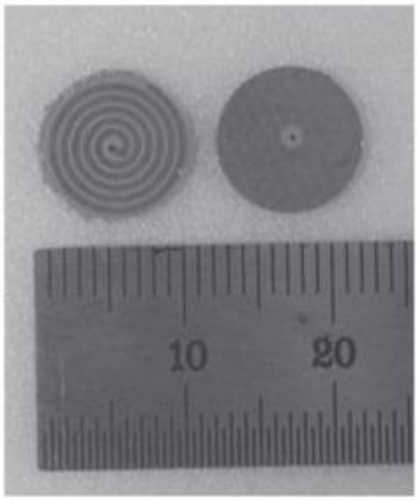

Figure 2.8: Spiral ingestible antenna designed for MICS band (taken from [20])

In [21] a helical antenna is suggested for the MICS frequency band. Similar to the last one, the helical shape causes a miniaturization of the antenna. This antenna measures 8 x 5.6 mm and it covers the MICS frequency band with a bandwidth of 32MHz.

In [22] a conformal antenna for the 915 MHz ISM band is presented. The antenna can be wrapped around the capsule inner wall with good performance while taking less space. The measured results show a bandwidth of 50 MHz. The suggested antenna is shown in figure 2.9.

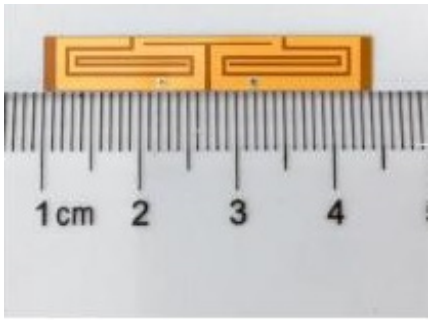

(a) Conformal antenna unwrapped

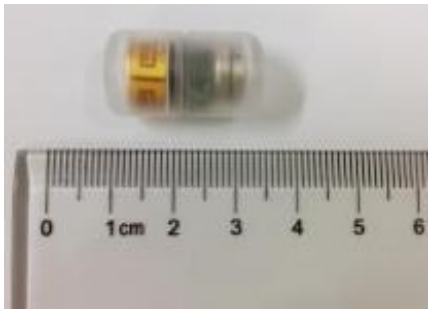

(b) Conformal antenna wrapped around capsule

Figure 2.9: Conformal patch ingestible antenna designed for the 915 MHz ISM band (taken from [22])

In [23] a meandered conformal antenna (figure 2.10) is suggested for the 433 MHz ISM frequency band. The antenna size is 36 x 21 mm and it has 124 MHz of bandwidth. The antenna shows a omni-directional radiation pattern necessary for ingestible antennas.

Figure 2.10: Conformal patch ingestible antenna designed for the 433MHz ISM band (taken from[23])

In [24] researchers design a meandered antenna for the WMTS frequency band. The antenna has a bandwidth of 200 MHz. The antenna's dimensions are 25 x 15 x 0.127 mm. This antenna is shown in figure 2.11

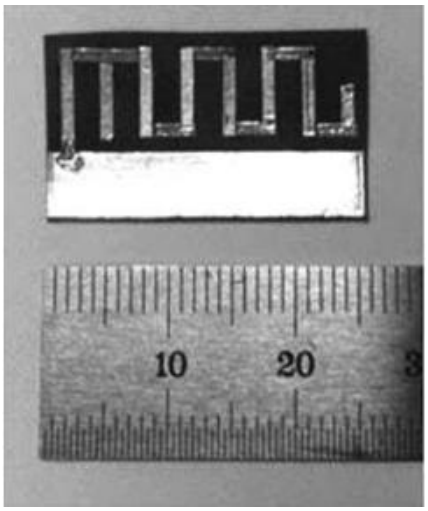

(a) Meandered antenna unwrapped

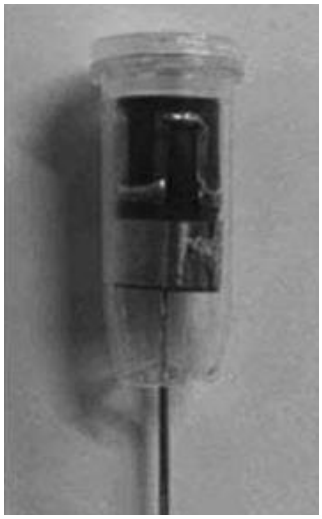

(b) Meandered antenna wrapped around capsule

Figure 2.11: Meandered antenna designed for the WTMS frequency band (taken from [24])

In [25] researchers propose a miniature microstrip antenna for the ISM frequency band. The antenna uses dielectric loading in order to achieve a fairly small dimension of 17 x 7 mm. The antenna is shown in figure 2.12

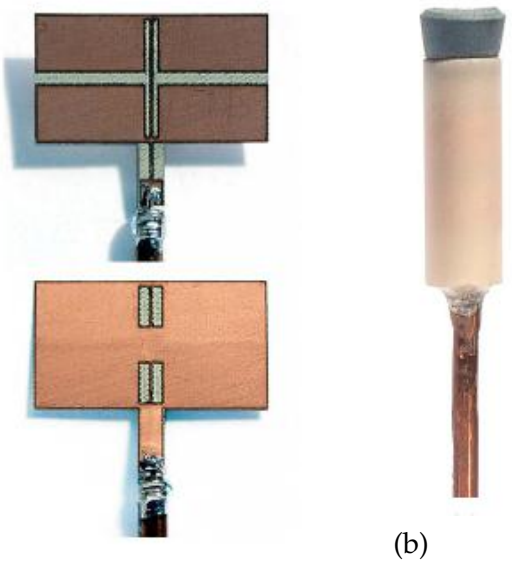

(a) Top/Back view (b) Wrapped

Figure 2.12: Wrapped micostrip antenna for the ISM frequency band(taken from [25])

In [26] researchers propose a miniature antenna that performs well in the 400 MHz ISM frequency band. The antenna substrate is polyimide due to its flexible material. The meandered design and the effects of the human body help miniaturize this antenna to a dimension of 30.2 x 11.2 mm as shown in figure 2.13.

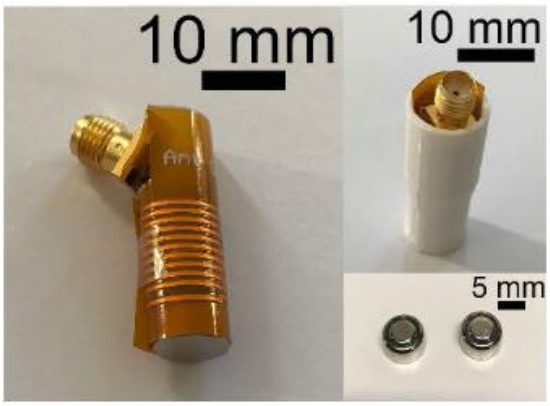

Figure 2.13: Meandered conformal antenna designed for the 433MHz ISM band (taken from [26])

Table 2.2: Ingestible antennas present in literature

Ingestible Antennas				
Antenna Type	*Bandwidth (MHz)*	*Size (mm)*	*Frequency band*	*Citation*
Spiral	70	10.1 x 10.1	MICS	[20]
Helical	32	8 x 5.6	MICS	[21]
Conformal	50	32 x 5.8	WMTS	[22]
Conformal	124	36 x 21	ISM	[23]
Microstrip	30	17 x 7	ISM	[25]
Meandered	—	30.2 x 11.2	ISM	[23]
Meander	150	25 x 10 x 0.125	WMTS	[24]

3

In-body antenna

As mentioned before, the goal of this thesis is to design an in-body antenna for the 2.45 GHz ISM band to communicate with an exterior antenna placed on the body. Since microstrip antennas are widely available and easy to manufacture, it will be the first option studied. In this chapter the design of an antenna for in-body applications will be presented.

At the start, a rectangular microstrip antenna will be considered. The design will consider free-space around the antenna and afterwards a homogeneous phantom will be added to test its performance. Following this step a superstrate will be added to the antenna in order to improve perfomance. Different materials will be tested as superstrate.

3.1 Antenna in free space

In order to simplify the process of designing the antenna, a basic rectangular microstrip antenna will be considered, as shown in figure 3.1.

The antenna will be made with a layer of dielectric material between two layers of electric conductor. The dielectric used will be FR-4, since its cheap and broadly utilized.

In order to have the best input match at 2.45 GHz, the antenna has the dimensions presented in table 3.1. These dimensions were calculated using equations present in

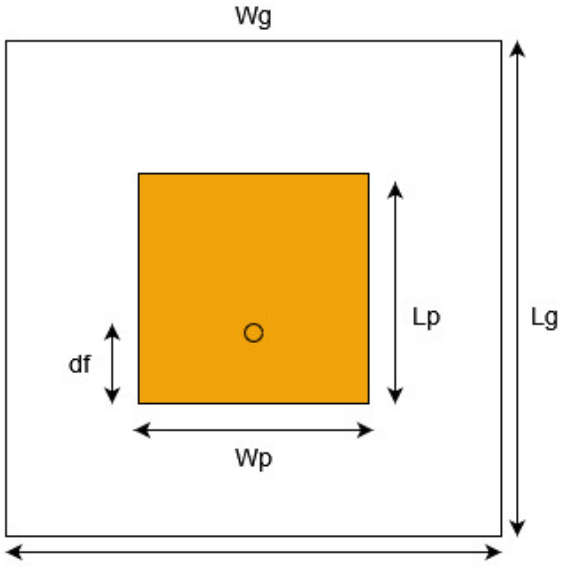

(a) Front view

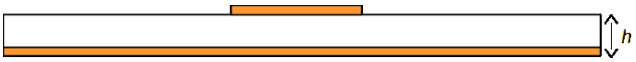

(b) Side view

Figure 3.1: Geometry of a microstrip antenna

literature [27] and are shown in equations 3.1, 3.2, 3.3 and 3.4. The results were further optimized in order to obtain the best input match level.

$$L_p = \frac{c}{2 \times f \times \sqrt{\varepsilon_r}} \tag{3.1}$$

$$\varepsilon_{ref} = \frac{\varepsilon_r + 1}{2} + \frac{\varepsilon_r - 1}{2} \times (1 + 12 \times \frac{h}{Wp})^{-\frac{1}{2}} \tag{3.2}$$

$$L_p = L_{eff} - 2 \times \Delta_L \tag{3.3}$$

$$\Delta_L = \frac{(\varepsilon_{ref} + 0.3) \times (\frac{W}{h} + 0.264)}{(\varepsilon_{ref} - 0.258) \times (\frac{W}{h} + 0.8)} \times 0.412h \tag{3.4}$$

Table 3.1: Antenna dimensions to be ressonant at 2.45 GHz

Wg	*Lg*	*Wp*	*Lp*	*df*
60mm	*60mm*	*30mm*	*28mm*	*7.5mm*

The theoretical input impedance and input match are shown in figure 3.2. The antenna peak performance is at ISM 2.45 GHz frequency band.

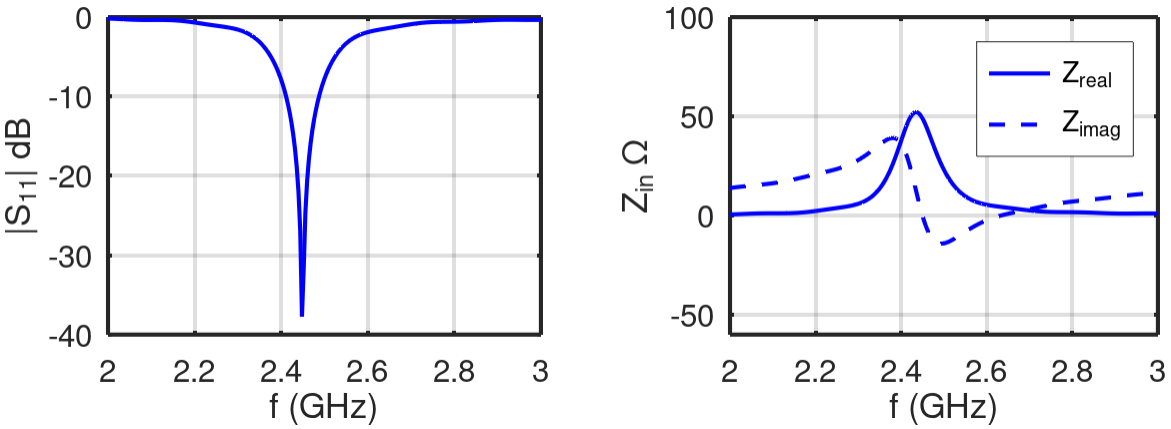

(a) Matching level

(b) Real and Imaginary impedance

Figure 3.2: Matching level and impedance for antenna in table 3.1

3.2 Phantom used in simulations

In this section the phantom used in simulations will be explained. To replicate testing conditions, the phantom has the same properties as pork muscle ($\varepsilon_r = 52.729$ and $\tan(\delta) = 0.24194$ at 2.45 GHz [28]) as this will be the material used to perform the measurements.

Table 3.2: Proposed Phantoms

Proposed Phantom	*Wc [mm]*	*Lc [mm]*	*Hc [mm]*
1	*100*	*150*	*25*
2	*120*	*200*	*40*
3	*170*	*250*	*60*

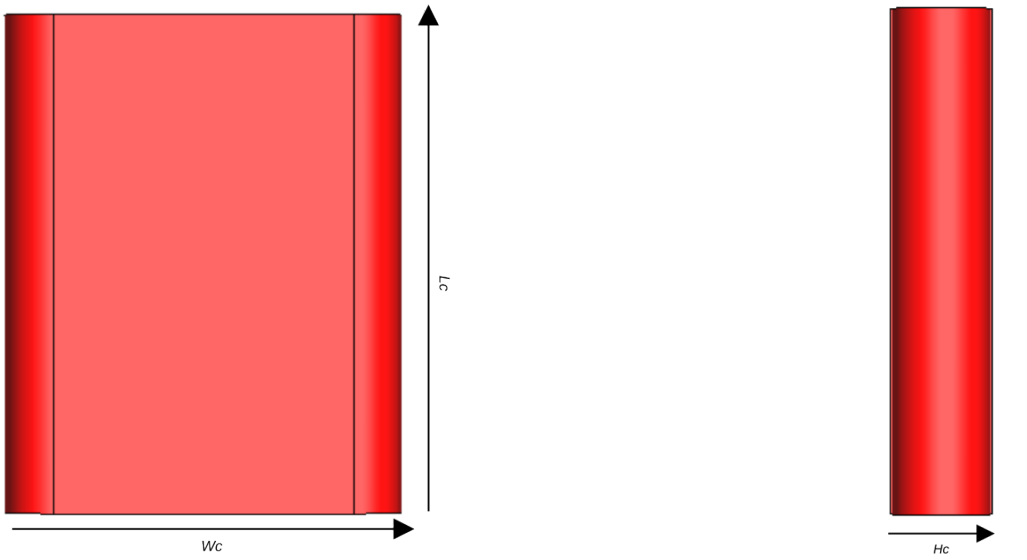

(a) Front View (b) Side View

Figure 3.3: Phantom used in simulations

Using the dimensions of a real human torso for the phantom would lead to long simulation time. A study was made in order to get the dimensions that would give accurate results but would decrease the simulation time. A table of proposed phantom dimensions is shown in table 3.2.

The previous antenna was placed inside the phantom in order test the results for all simulated proposed phantoms. The results are shown in figure 3.4. The increase in dimensions from phantom 1 to phantom 2 impacted results however, the increase in dimensions from phantom 2 to phantom 3 did not cause significant effects. Because of this, phantom 2 was chosen as the preferred phantom, since the simulating time would be a lot shorter.

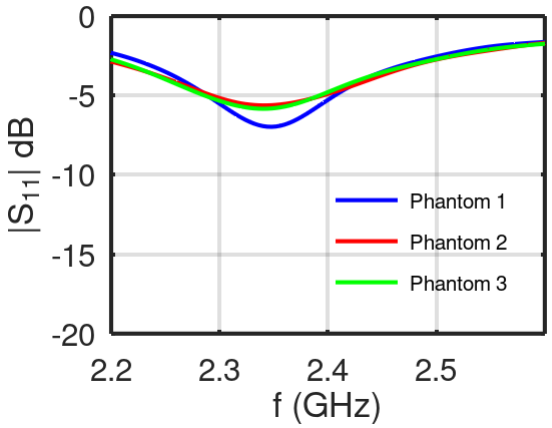

Figure 3.4: Study of proposed phantoms

3.3 Antenna inside phantom

The antenna must now be put inside the phantom to test its performance. For on-body applications a human body can be approximated by using a phantom with 2/3 of dielectric properties of muscle [5]. However, since we will use pork meat to test the antenna, and pork meat and human muscle have similar dielectric properties, the phantom will have the dielectric properties of human muscle to get the more accurate results as possible.

The antenna was affected by the phantom, as shown in figure 3.5. Impedance is not 50 Ω, even with the feed point near the border of the patch.

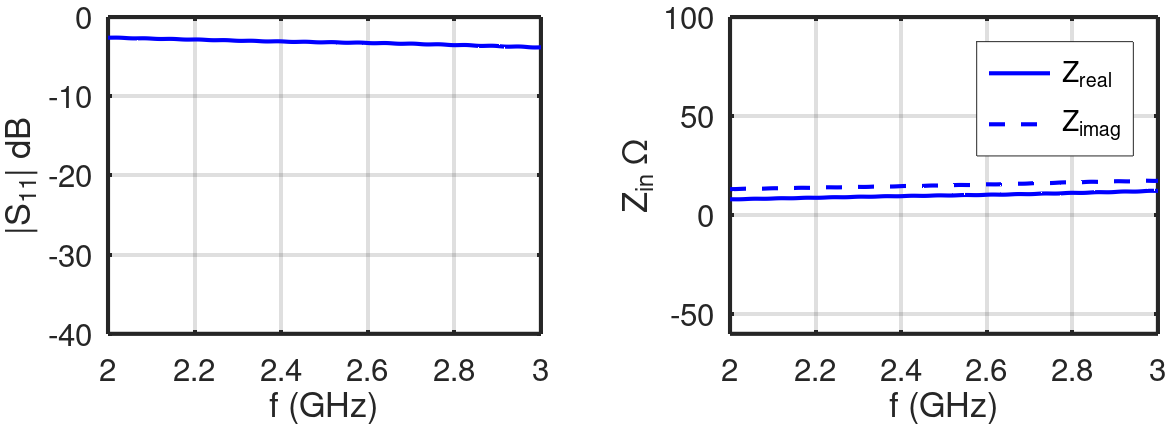

(a) Matching level

(b) Real and Imaginary impedance

Figure 3.5: Matching level and impedance for antenna inside phantom

The use of a superstrate has been shown to decrease coupling between the antenna and biological tissues [29] and may provide a solution.

3.3.1 Superstrate height impact on the antenna performance

In order to study the impact of the superstrate height on the antenna perfomance, a layer of FR-4 was added to the antenna, as shown in figure 3.6. The results are shown in figure 3.7. The larger the superstrate height, the better antenna performance inside the phantom. However the superstrate addition causes a frequency shift requiring optimization in order to have it tunned at 2.45 GHz again.

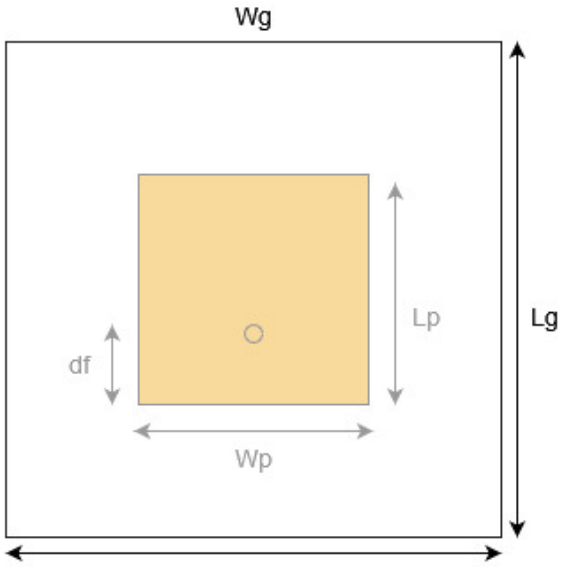

(a) Front view

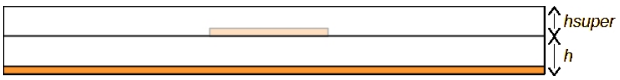

(b) Side view

Figure 3.6: Geometry of a microstrip antenna with superstrate

3.3.2 Superstrate material impact on the antenna performance

As the performance of the antenna depends on the properties of the materials used, several superstrate materials will be tested. Three different commercially available materials, presented in table 3.3, will be evaluated, all with a thickness of 3.2 mm. The input match obtained by simulation are shown in figure 3.8 where it can be seen that RT5880 is the material with best performance. The results seem to indicate that although the inclusion of a transition medium from the antenna to the body tissue

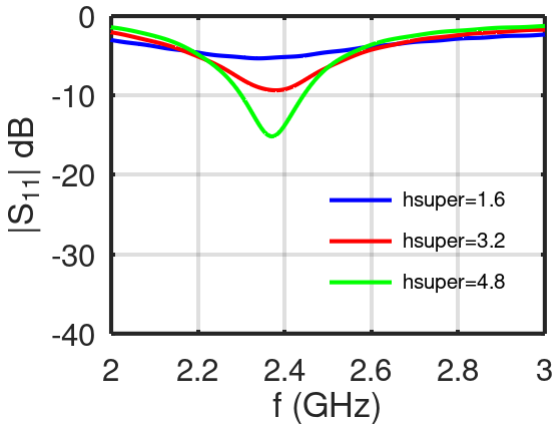

Figure 3.7: Effect of variable *hsuper* (dimensions in mm)

improves the antenna performance, this transition shouldn't be too sharp since the superstrate with the lowest permittivity provided the best results.

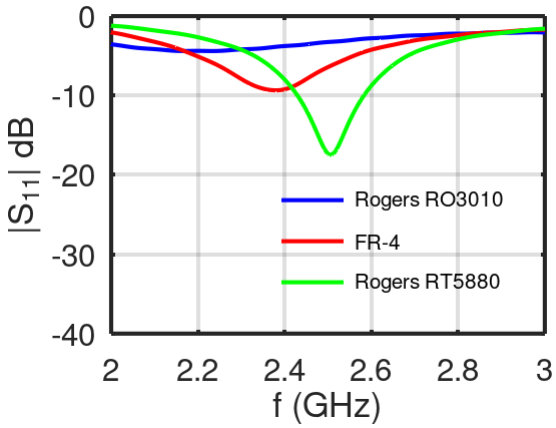

Figure 3.8: Matching level for different materials inside phantom

Table 3.3: Materials used

Material Name	*Permittivity*	*Loss tangent*
FR-4	4.3	0.025
Rogers RT5880	2.2	0.0009
Rogers RO3010	11.2	0.0021

3.3.3 Optimized antenna inside the phantom

Based on the previous sections, a new antenna was designed with dimensions presented in table 3.4. The antenna material consists of FR-4 and Rogers RT5880 for substrate and superstrate, respectively. The antenna shows a reflection coefficient of -22.7 dB at 2.45 GHz and covers the whole 2.45 GHz ISM band with 182 MHz of bandwidth as shown in figure 3.9. This configuration is shown in figure 3.10.

Table 3.4: Antenna dimensions to be optimized for 2.45 GHz inside phantom

Wg	*Lg*	*Wp*	*Lp*	*hsuper*	*df*
60mm	*60mm*	*25mm*	*28.75mm*	*3.2mm*	*2mm*

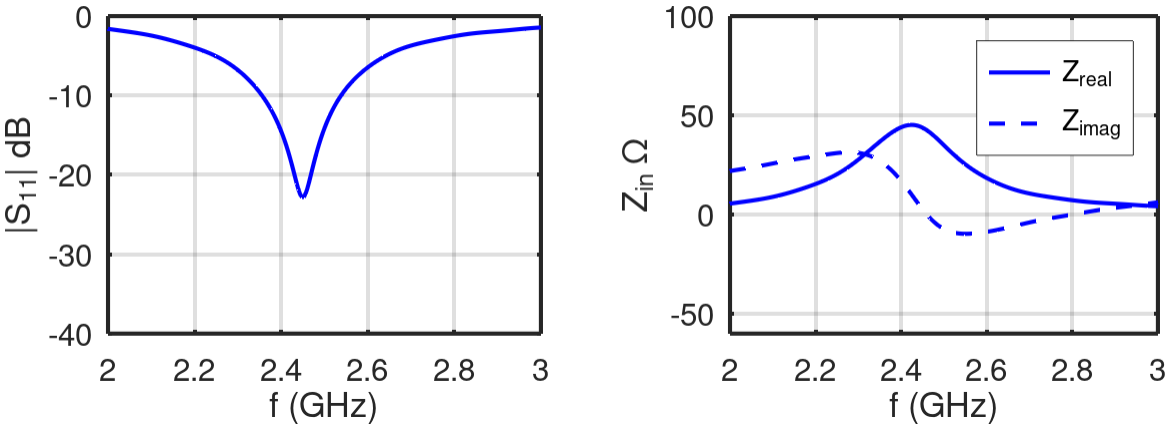

(a) Matching level

(b) Real and Imaginary impedance

Figure 3.9: Matching level and impedance for optimized antenna inside phantom

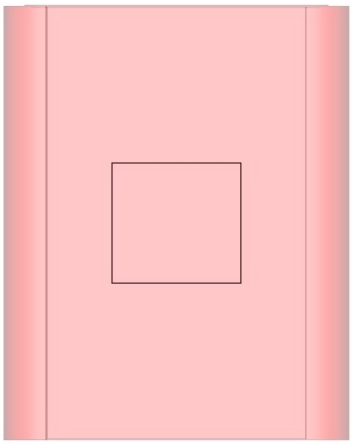

(a) Front view

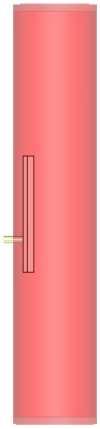

(b) Side view

Figure 3.10: Optimized antenna inside phantom

While the antenna has robust performance for the 2.45 GHz ISM frequency band, the dimensions are far too big for an in-body antenna. In the next chapter miniaturization techniques will be studied in order to compact the antenna.

4

Miniaturization Techniques for Microstrip Antennas

In this chapter miniaturization techniques will be studied in order to compact the antenna suggested in the previous chapter. In [30] miniaturization techniques are discussed for microstrip antennas. In this document three will be studied:

- Increase the permittivity of substrate material;
- Addition of slits in ground plane or in the patch;
- Addition of shorting pins.

These techniques will first be studied with the antenna from table 3.1 operating in free-space.

4.1 Increase the permittivity of substrate material

Antennas can be compacted with the use of a higher permittivity material as substrate [27]. For this study FR-4 substrate was changed to Rogers RO3010. This material has a dielectric constant $\varepsilon_r = 11.2$. Simulation results conducted with this material showed a frequency shift to 1.55 GHz as shown in figure 4.1. However, the change of material also affected antenna matching, with impedance values being 120-j36 Ω.

Table 4.1: Antenna dimensions optimized for 2.45 GHz with Rogers RO3010 (ε_r =11.2) as substrate

Wg	*Lg*	*Wp*	*Lp*	*df*
35mm	35mm	27.5mm	17mm	5.5mm

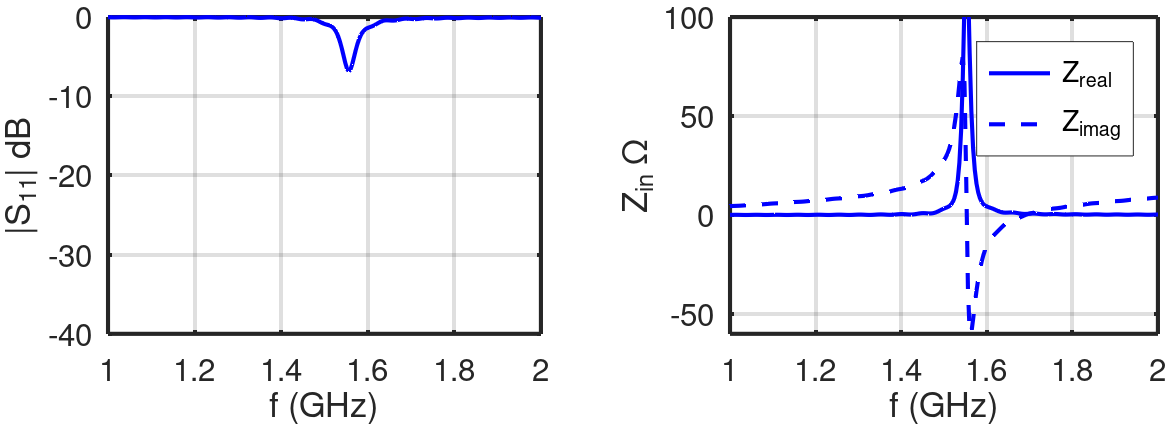

(a) Matching level (b) Real and Imaginary impedance

Figure 4.1: Matching level and impedance for antenna with Rogers RO3010 (ε_r =11.2) as substrate

Antenna dimensions need to be shortened in order to have a good performance at the 2.45 GHz ISM frequency band. Final antenna dimensions are shown in table 4.1. Simulated results are shown in figure 4.2. The antenna shows good performance for the 2.45 GHz ISM frequency band. However, bandwidth suffered as the antenna is only capable of performing within 31 MHz.

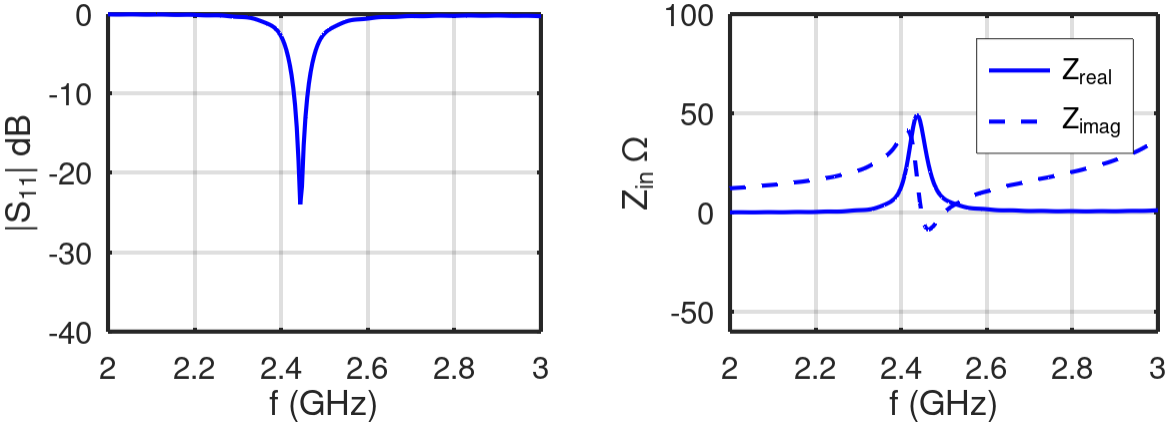

(a) Matching level (b) Real and Imaginary impedance

Figure 4.2: Matching level and impedance for compacted antenna with Rogers RO3010 (ε_r =11.2) as substrate

Table 4.2: Bandwidth for each substrate height

Substrate Height	*Bandwidth*
1.6 mm	32 MHz
3.2 mm	49 MHz
4.8 mm	57 MHz

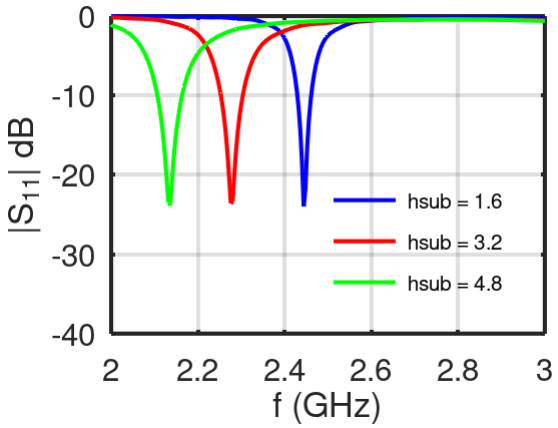

Figure 4.3: Effect of variable hsub (substrate height)

Bandwidth can be enhanced by increasing the substrate height [30]. This may provide a solution to cover the whole ISM 2.45 GHz frequency band. Simulations were conducted in order to study the effect of substrate height on bandwidth and results are present in figure 4.3. Substrate height causes a shift to a lower frequency which can be exploited to further miniaturize the antenna. Bandwidths for each substrate height are presented in table 4.2. Bandwidth is enhanced but its not enough to cover the whole ISM 2.45 GHz frequency band. This however might change inside the phantom, since the losses caused by it will enhance antenna bandwidth.

By placing this antenna inside the phantom and optimizing its dimensions we can achieve the results present in figure 4.4. Antenna dimensions are presented in table 4.3. The antenna presents a bandwidth of 144 MHz, covering the whole 2.45 ISM frequency band.

Table 4.3: Antenna dimensions in order to be resonant at 2.45 GHz with Rogers RO3010 as substrate inside the phantom

Variable	*Dimension (mm)*
Lg	35
Wg	35
Lp	18.2
Wp	19
df	2
h	1.6
hsuper	3.2

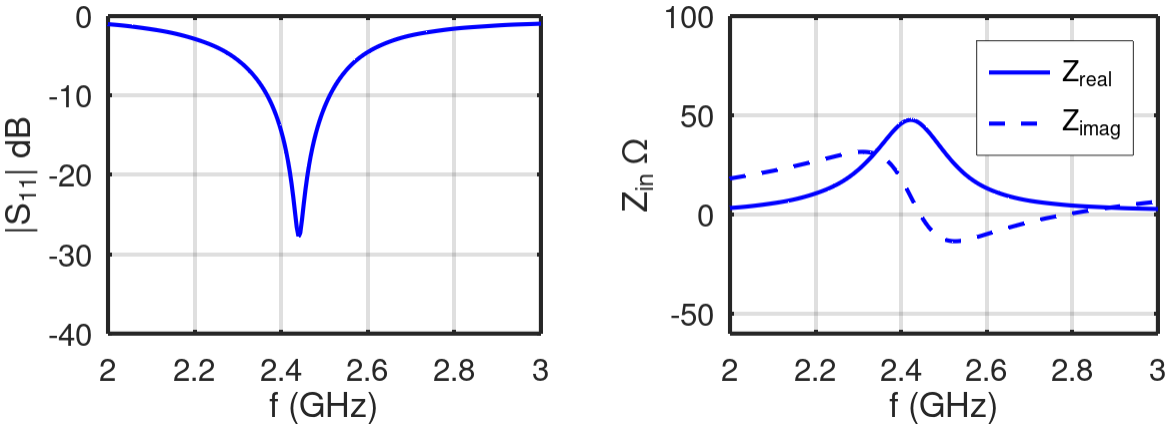

(a) Matching level

(b) Real and Imaginary impedance

Figure 4.4: Matching level and impedance for compacted antenna with Rogers RO3010 (ε_r =11.2) as substrate inside the phantom

4.2 Adding slits to the antenna

Another method of compacting the antenna is with the use of slits. Slits can be added in either the ground plane or patch. Slits compact the antenna by modifying the flow of electric current. The study will be done in three parts:

1. First we will study the effect of slits on the ground plane and study how slit length and width affect the antenna. The antenna will be compacted until the frequency reaches 2.45 GHz;

2. Next we will add a superstrate and study the effects of the slits with the superstrate and resize the antenna to 2.45 GHz;

3. Finally we will place the compacted antenna inside the phantom and do the resizing necessary to bring the antenna back to 2.45 GHz.

After this study is done we will repeat the process for the slits in the patch.

4.2.1 Slits in ground plane

In this section the effects of slits in the ground plane will be studied. As usual, the base antenna is the one designed for free-space. Slits will have the dimensions of table 4.4 and will be added to the antenna as shown in figure 4.5.

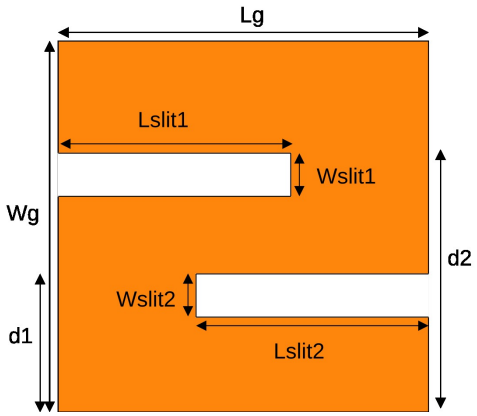

Figure 4.5: Geometry of antenna with slits in ground plane

Table 4.4: Slit dimensions in mm

Wslit1	*LSlit1*	*Wslit2*	*LSlit2*	*Lg*	*Wg*	*D1*	*D2*
1	30	1	30	60	60	9.33	18.66

In figure 4.6 simulation results are shown. Slits in the ground plane are very effective at compacting the antenna. The addition of slits resulted in a frequency shift to 1.23 GHz.

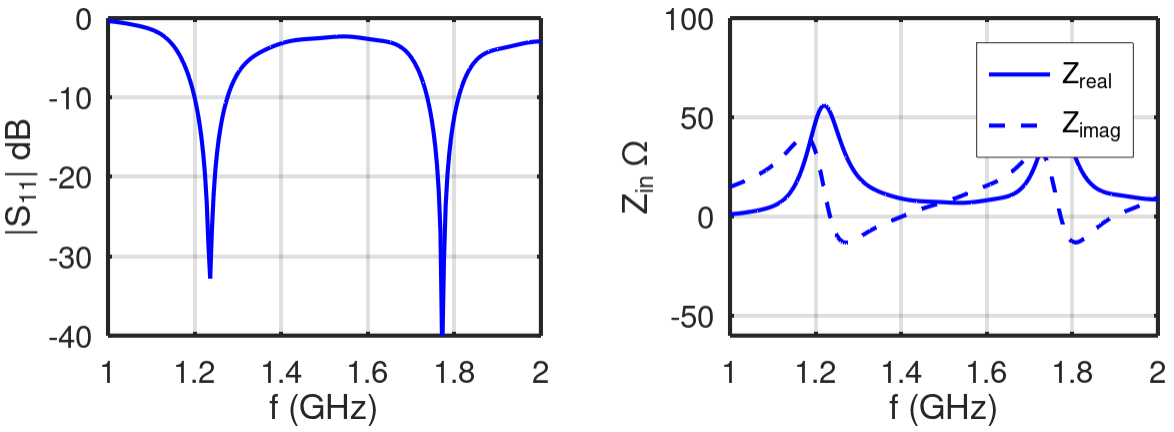

(a) Matching level (b) Real and Imaginary impedance

Figure 4.6: Matching level and impedance for antenna with dimensions of table 3.1 with slits in ground plane

A parametric study was done in order to understand how the variables affect antenna performance. Position of both slits was fixed, since it is common to partition the antenna equally. Simulations results are shown in figure 4.7. The longer the slit, the larger the frequency shift, which can be used to further compact the antenna. Bandwidth also increases with the increase of the length and width of the slit. This behavior is due to the increase of losses caused by the addition of the slits [30].

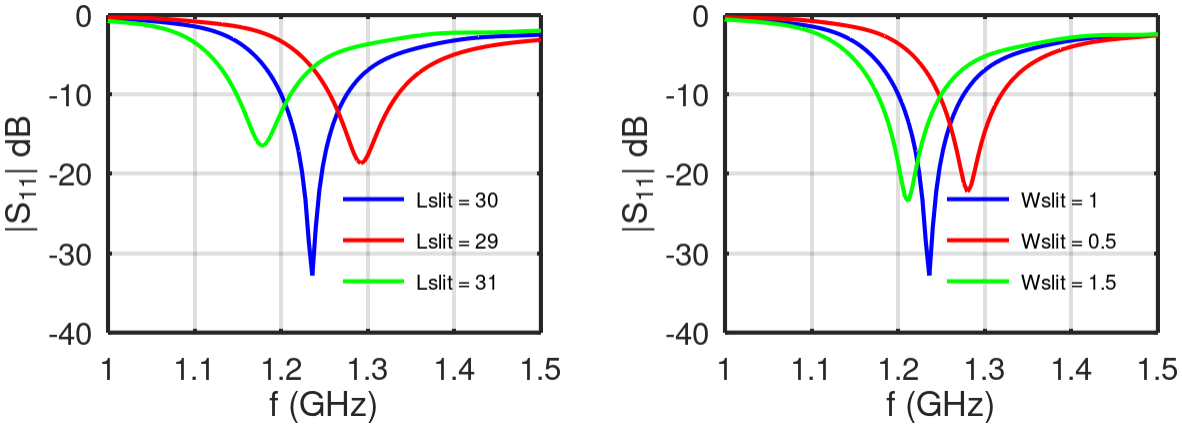

(a) Effect of variable LSlit (b) Effect of variable WSlit

Figure 4.7: Parametric study of slits in ground plane (dimensions in mm)

With slits in the ground plane we can compact the antenna to the dimensions of table 4.5. Results are shown in figure 4.8. Although the antenna is much smaller with the use of slits, the bandwidth is reduced to only 60 MHz.

Table 4.5: Antenna dimensions in order to be resonant at 2.45 GHz with slits in ground

Variable	*Dimension (mm)*	*Variable*	*Dimension (mm)*
Lg	20	Lslit	9
Wg	20	Wslit	1
Lp	15	d1	5
Wp	16	d2	10
df	6.5	h	1.6
xf	3.5		

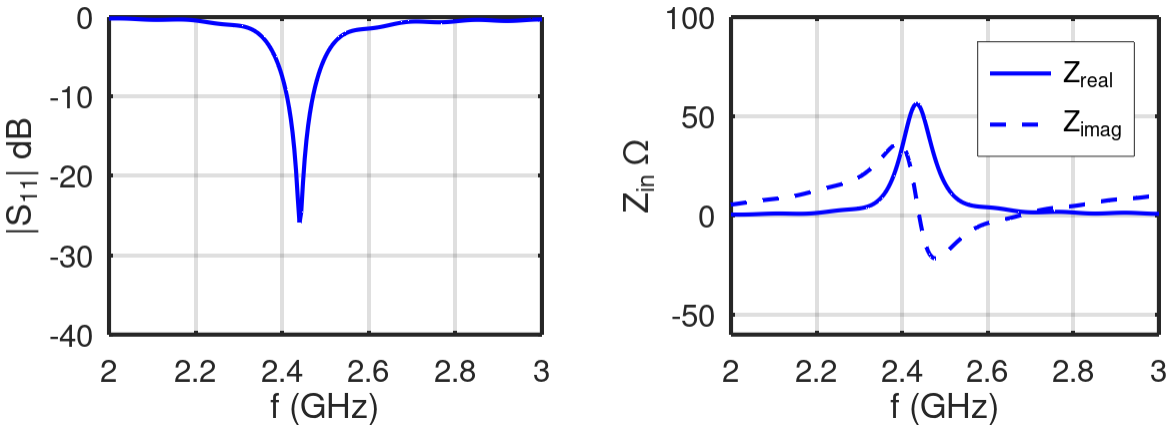

(a) Matching level

(b) Real and Imaginary impedance

Figure 4.8: Matching level and impedance for compacted antenna with slits in ground

As said before, slits change the current flow, allowing for the miniaturization of the antenna. This is shown in figure 4.9.

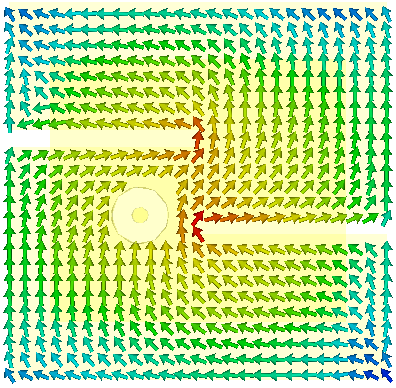

Figure 4.9: Current distribution of antenna with slits in ground

A superstrate was added in order to study its effects on the antenna with slits. Results are shown in figure 4.10. The antenna's frequency shifts to 1.21 GHz.

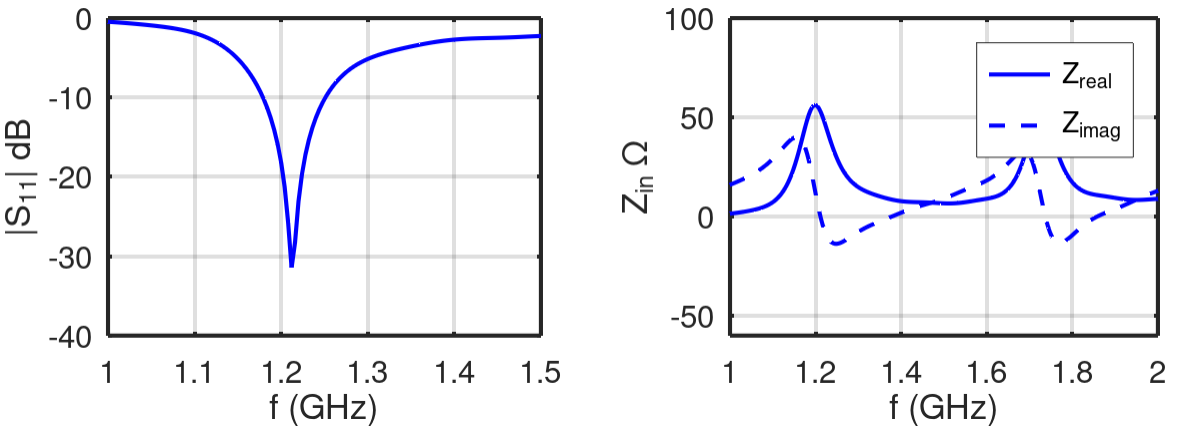

(a) Matching level (b) Real and Imaginary impedance

Figure 4.10: Matching level and impedance for antenna with slits in ground with superstrate

A parametric study was done in order to evaluate if the behavior with the addition of the superstrate is the same as the behavior without it. Simulated results are shown in figure 4.11. With superstrate the frequency shift is larger.

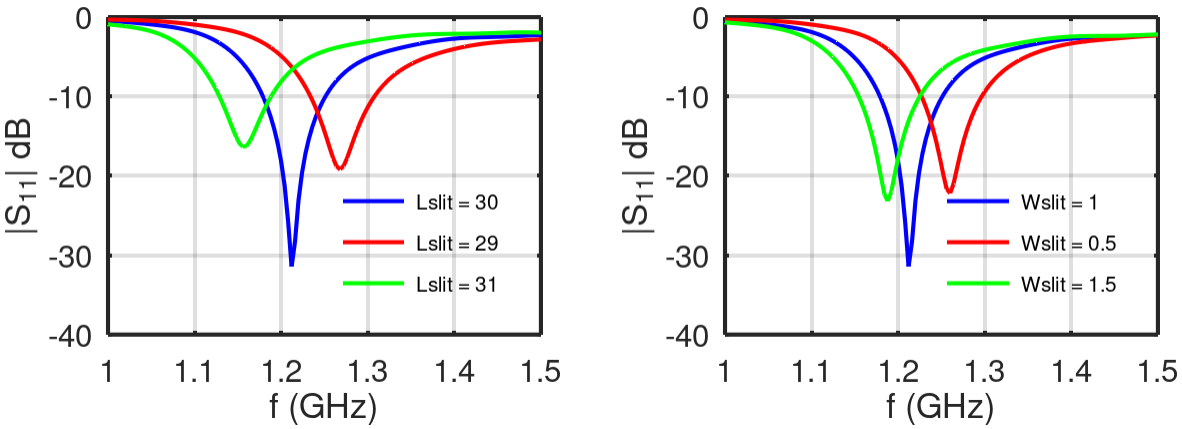

(a) Effect of variable LSlit (b) Effect of variable WSlit

Figure 4.11: Parametric study of slits in ground plane with superstrate

The antenna can be compacted to the dimensions of table 4.6. Simulation results are shown in figure 4.12. Although the antenna doesn't have enough bandwidth in free-space, inside the phantom the behavior will be different due to the losses caused by the phantom.

Table 4.6: Antenna dimensions in order to be resonant at 2.45 GHz with slits in ground with superstrate

Variable	*Dimension (mm)*	*Variable*	*Dimension (mm)*
Lg	20	Lslit	9
Wg	20	Wslit	1
Lp	13.5	d1	5
Wp	16	d2	10
df	6.5	h	1.6
xf	4	hsuper	1.6

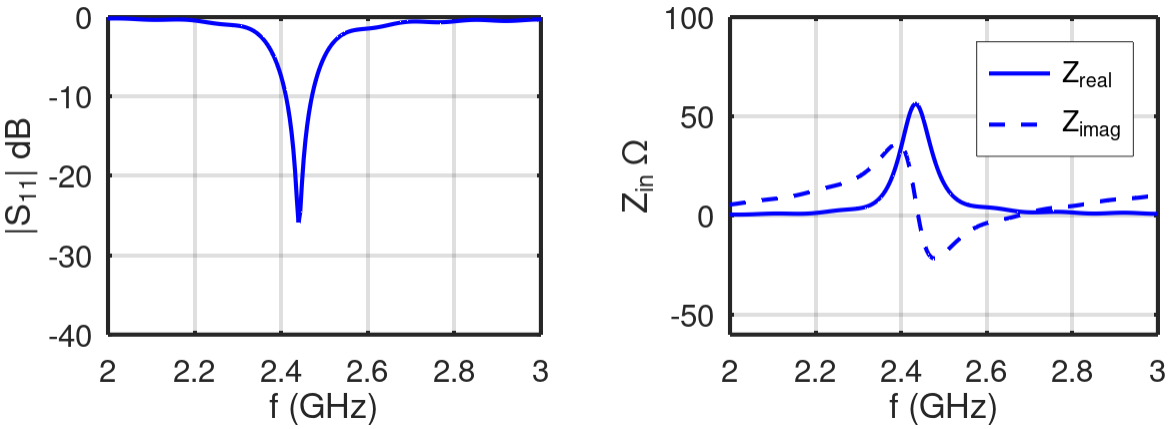

(a) Matching level

(b) Real and Imaginary impedance

Figure 4.12: Matching level and impedance for compacted antenna with slits in ground

When this antenna is placed inside the phantom however, the coupling caused by the phantom detunes the antenna. No feeding point was able to feed the antenna with 50 Ω of impedance. Simulated results are shown in figure 4.13.

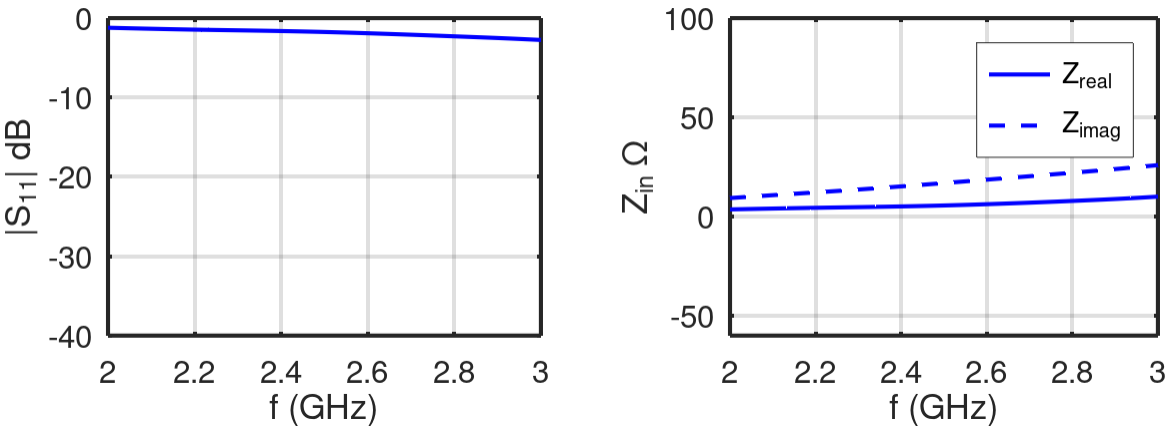

(a) Matching level (b) Real and Imaginary impedance

Figure 4.13: Matching level and impedance for antenna with slits in the ground plane inside the phantom

These results exclude the option of adding slits to the ground of the antenna in order to compact it.

4.2.2 Slits in patch

In this section the effect of slits in the patch will be studied. Slits will have the dimensions of table 4.7. As usual, the base antenna will be the designed for free-space.

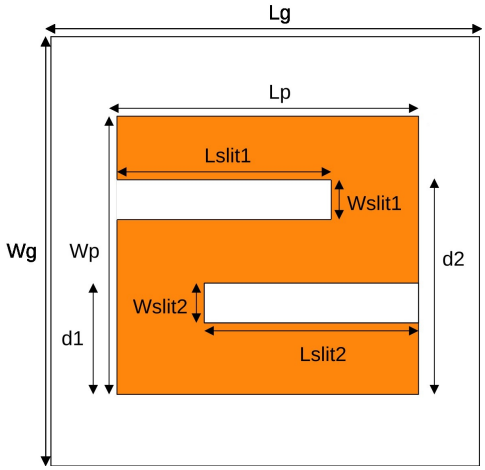

Figure 4.14: Geometry of antenna with slits in patch

Table 4.7: Slit dimensions in mm

Wslit1	*LSlit1*	*Wslit2*	*LSlit2*	*D1*	*D2*
1	10	1	10	9.33	18.66

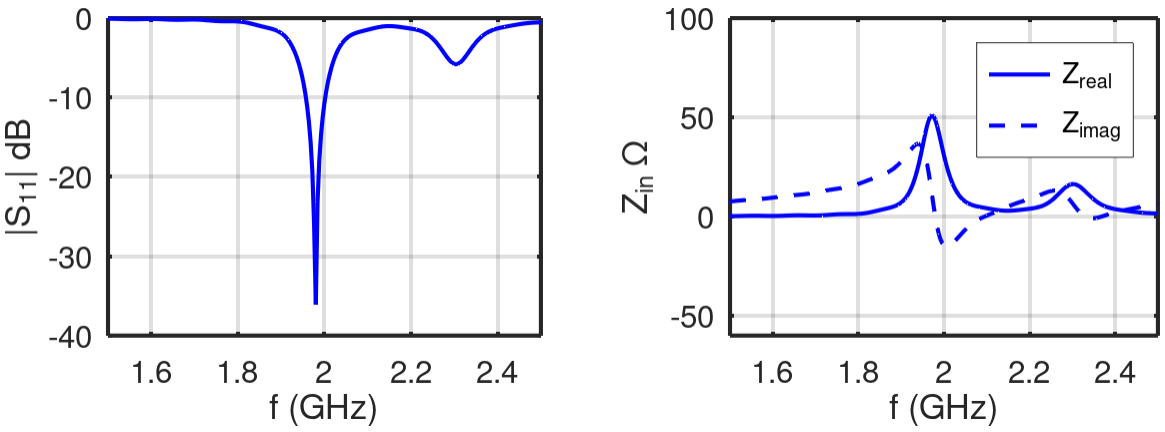

(a) Matching level (b) Impedance

Figure 4.15: Matching level and impedance for antenna with slit dimensions of table 4.7

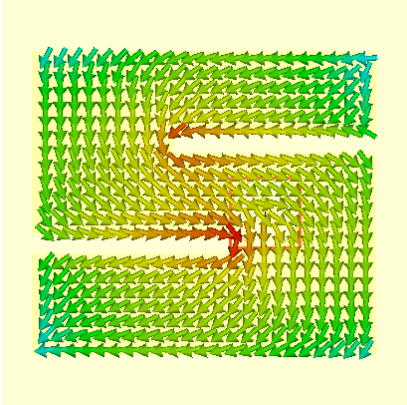

Figure 4.16: Current distribution of antenna with slits in patch

Simulated results are shown in figure 4.15. The slits in the patch caused a frequency shift to 1.98 GHz. Bandwidth is severely affected however, with the antenna only performing within 44 MHz. Slits in the patch are not as effective as compacting the antenna as slits in the ground. Although slits have different dimensions, they "end" in the same place. This is because the slit in the ground plane begins in the edge of the ground plane, and slits in the patch begin in the edge of the patch. Another observation we can make is the deterioration of bandwidth. Unlike slits in the ground plane, slits in the patch result in a bandwidth decrease. Current distribution is shown in figure 4.16

A parametric study was done in order to understand how the variables affect antenna performance. Simulations results are shown in figure 4.17. The lengthier the slit, the larger the frequency shift, which can be used to further compact the antenna. This however affects bandwidth, with a lengthier slit resulting in a decrease of bandwidth.

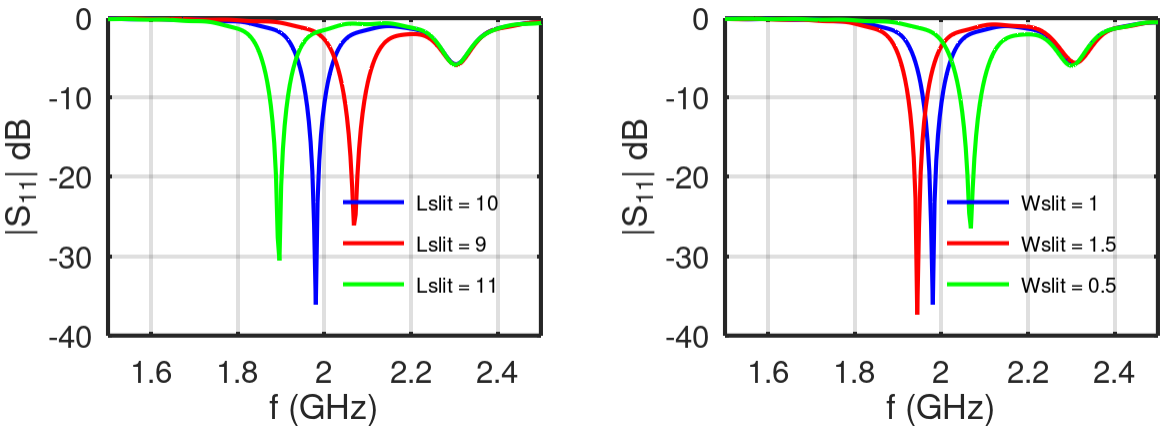

(a) Effect of variable LSlit

(b) Effect of variable WSlit

Figure 4.17: Parametric study of slits in patch

Table 4.8: Antenna dimensions in order to be resonant at 2.45 GHz with slits in patch

Variable	*Dimension (mm)*	*Variable*	*Dimension (mm)*
Lg	20	Lslit	10
Wg	20	Wslit	1
Lp	15	d1	5
Wp	17	d2	10
df	7	h	1.6
xf	3		

The same principle applies to the width of the slit.

With the use of slits we can compact the antenna to the dimensions of table 4.8, with the results shown in figure 4.18.

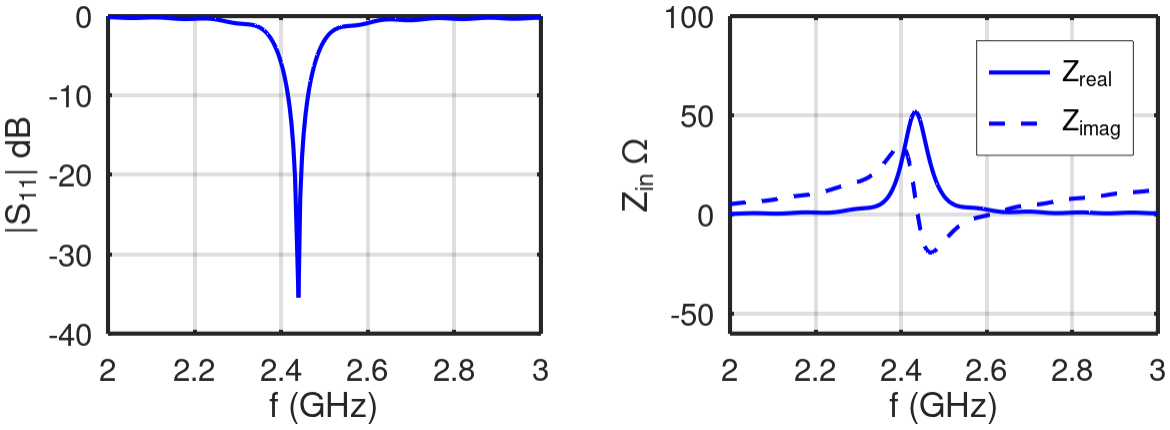

(a) Matching level

(b) Real and Imaginary impedance

Figure 4.18: Matching level and impedance of antenna with dimensions of table 4.8

Table 4.9: Antenna dimensions in order to be resonant at 2.45 GHz with slits in patch with superstrate

Variable	*Dimension (mm)*	*Variable*	*Dimension (mm)*
Lg	18	Lslit	9.5
Wg	18	Wslit	1
Lp	13.75	d1	4.58
Wp	15	d2	9.16
df	7	h	1.6
xf	3	hsuper	1.6

Although the antenna is much more compact with the use of slits, bandwidth is severely affected with the antenna presenting only 45 MHz.

Again, slit effects with superstrate must also be studied, since the goal is to compact the antenna inside the phantom and the use of the superstrate is essential. A parametric study was done, with a superstrate in the antenna. Results are shown in figure 4.19.

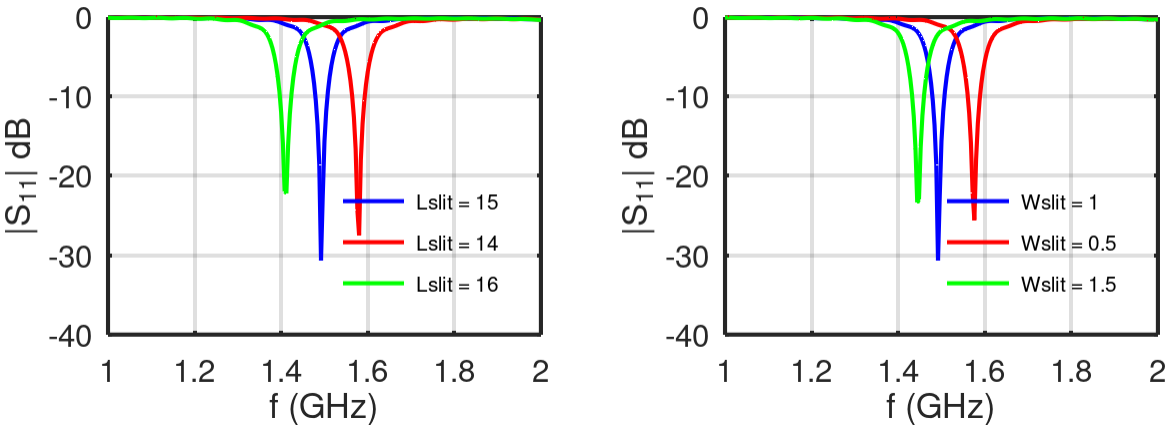

(a) Effect of variable LSlit

(b) Effect of variable WSlit

Figure 4.19: Parametric study of slits in patch with superstrate

The superstrate shifts the antenna to a lower frequency, which is useful for our goal. Bandwidth is even smaller with the use of superstrate however. With the superstrate we can compact the antenna to the dimensions of table 4.9. Results are shown in figure 4.20.

The antenna with superstrate is more compact. However, bandwidth is only 40 MHz. Although this antenna doesn't have enough bandwidth in free-space, as seen previously, the placement of the antenna inside the phantom will increase the bandwidth.

After optimizing the antenna to work inside the phantom we get the results of figure 4.21 with the dimensions of table 4.10. Antenna was further compacted due to the

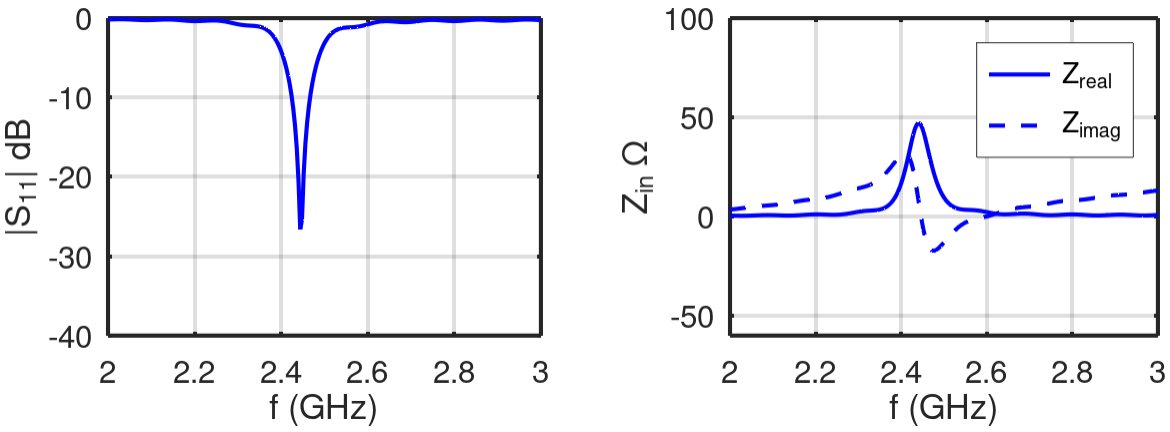

(a) Matching level (b) Impedance

Figure 4.20: Matching level and impedance for antenna with dimensions of table 4.9

Table 4.10: Antenna dimensions in order to be resonant at 2.45 GHz with slits in patch with superstrate

Variable	*Dimension (mm)*	*Variable*	*Dimension (mm)*
Lg	16	Lslit	8.45
Wg	16	Wslit	1
Lp	13	d1	4
Wp	13	d2	8
df	4.6	h	1.6
xf	3	hsuper	1.6

high permittivity of the phantom and bandwidth was enhanced to a value of 126 MHz, covering the whole 2.45 GHz ISM frequency band. The antenna inside the phantom is shown in figure 4.22

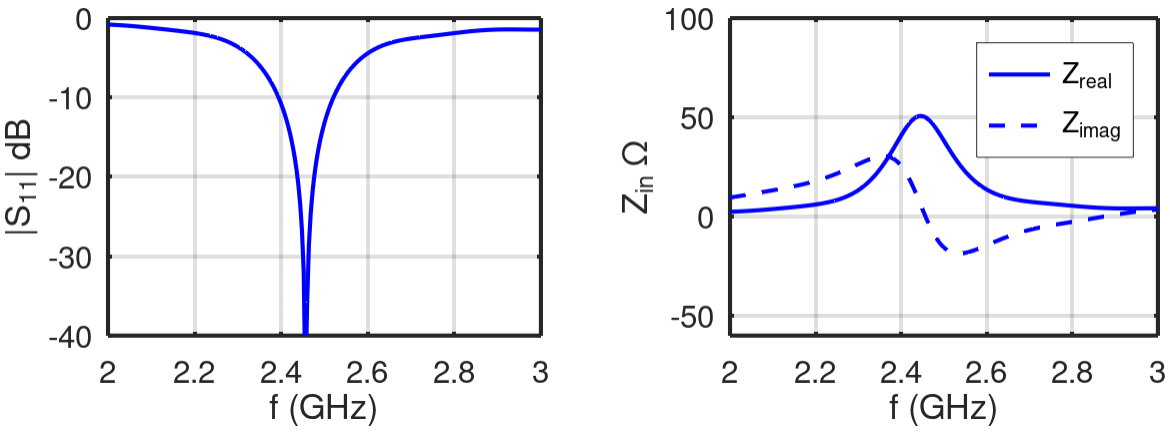

(a) Matching level (b) Impedance

Figure 4.21: Matching level and impedance for antenna with dimensions of table 4.10

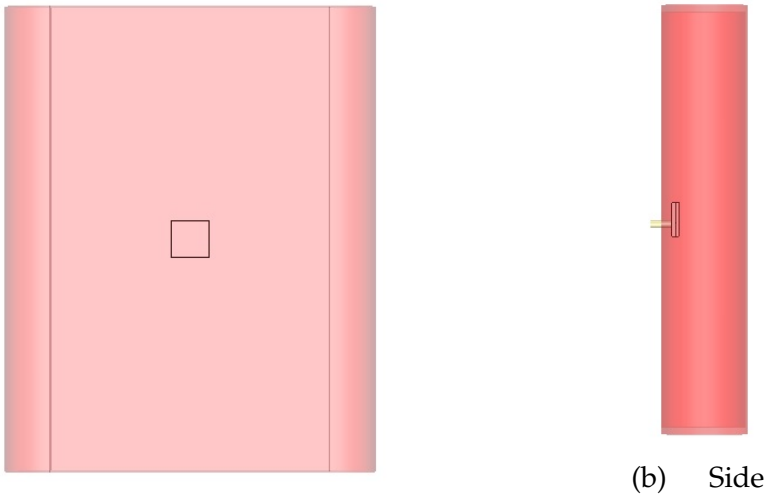

(a) Front view (b) Side view

Figure 4.22: Optimized antenna inside phantom with slits

4.3 Adding shorting pins to the antenna

Another technique to compact antennas is the use of a shorting pin. The following effects will be studied:

1. The effects of a single shorting pin on the base antenna;
2. The effects of multiple shorting pins on the base antenna;
3. The effects of the size of the shorting pins;
4. The effects of the position of the shorting pins and the distance between them.

Following this a superstrate will be added and the study will be repeated.

A shorting pin was added to the base antenna as illustrated in figure 4.23 with the shorting pin dimensions presented in table 4.11. The input match obtained by the simulation results are shown in figure 4.24 and the results show a frequency shift to 820 MHz enabling a very effective miniaturization of the antenna. This miniaturization however comes at the cost of bandwidth.

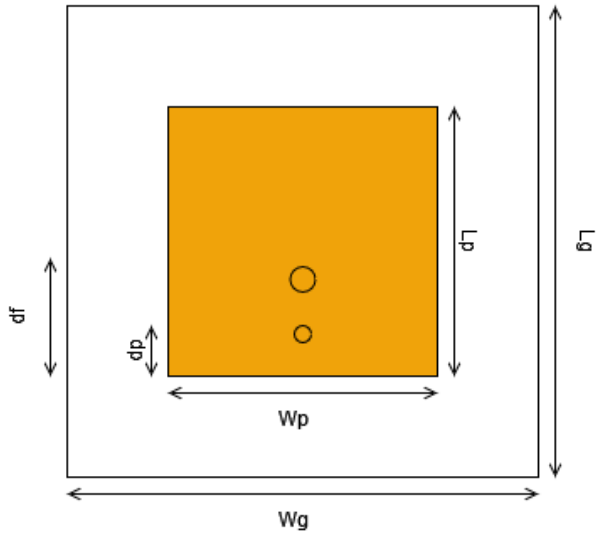

(a) Front view

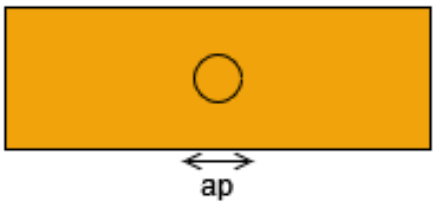

(b) Shorting pin zoomed in

Figure 4.23: Geometry of the antenna with one shorting pin

Table 4.11: Shorting pin dimensions

dp	*ap*
1 mm	0.4 mm

A parametric study of the variables will be done. Simulated results are shown in figure 4.25.

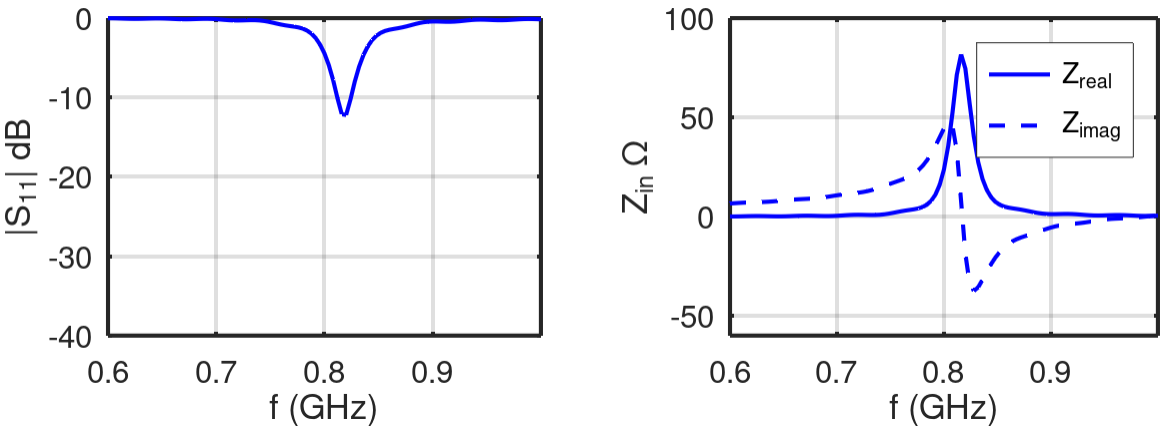

(a) Matching level (b) Impedance

Figure 4.24: Matching level and impedance for antenna with one shorting pin

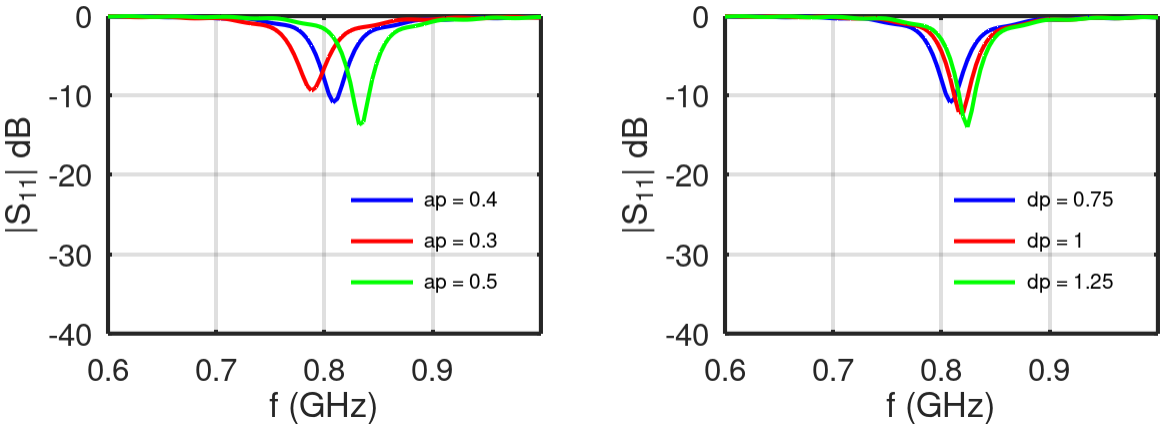

(a) Effect of pin diameter (b) Effect of pin position

Figure 4.25: Parametric study of shorting pins

The results of the parametric study indicate that the smaller the diameter of the shorting pin, the more effective it is at compacting the antenna. Similar behaviour happens with the distance from the edge of the patch. The smaller the distance, the more effective it is at compacting the antenna.

The addition of a shorting pin changes the current flow path, making the more optimal feed point very close to the shorting pin [30]. This behaviour makes it hard to feed the antenna with a standard connector. The addition of more shorting pins makes this optimal feed point further away, making it easier to feed the antenna. However, the effects of the quantity of shorting pins in the antenna must be studied.

In order to study these effects shorting pins were added to the antenna as illustrated in figure 4.26. Simulated results of the input match are shown in figure 4.27 and indicate

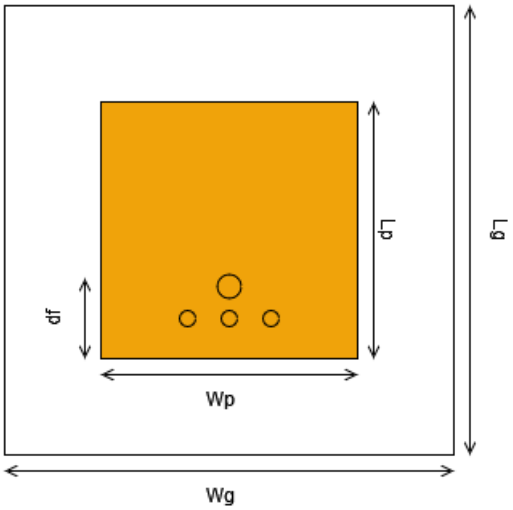

(a) Front view of in-body antenna

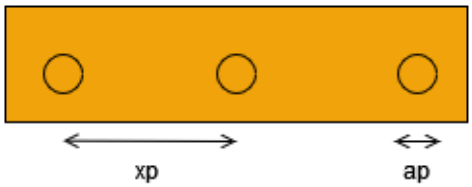

(b) Shorting pins zoomed in

Figure 4.26: Geometry of the antenna with three shorting pins

that the addition of shorting pins decreases the effects of miniaturization. This is necessary however to get the feed point further away from the shorting pin thus making it easier to feed the antenna.

A parametric study of the quantity of shorting pins and the distance between them is shown in figure 4.28. Results indicate that the further away the shorting pins are from each other, the less effective they are at compacting the antenna. For the design of this antenna three shorting pins will be used, since it's a balance between miniaturization and ease of feeding the antenna.

Next we will add a superstrate and study its effects on the antenna with a shorting pin. In order to do this, a parametric study of the diameter, the distance from the edge of the patch, and the distance between shorting pins was done. Simulated results are shown in figure 4.29 and indicate that, as usual, the addition of the superstrate shifts the antenna to a lower frequency.

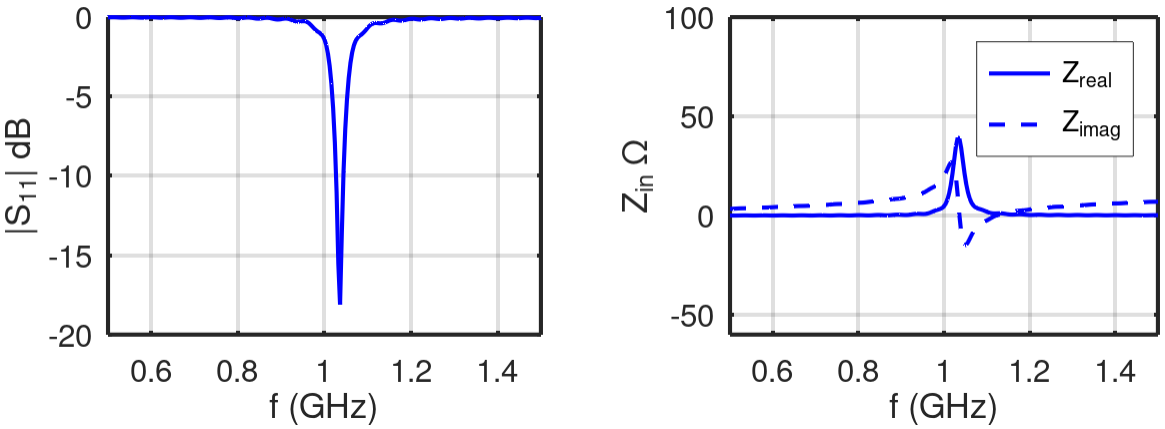

(a) Matching level (b) Impedance

Figure 4.27: Matching level and impedance for antenna with three shorting pins

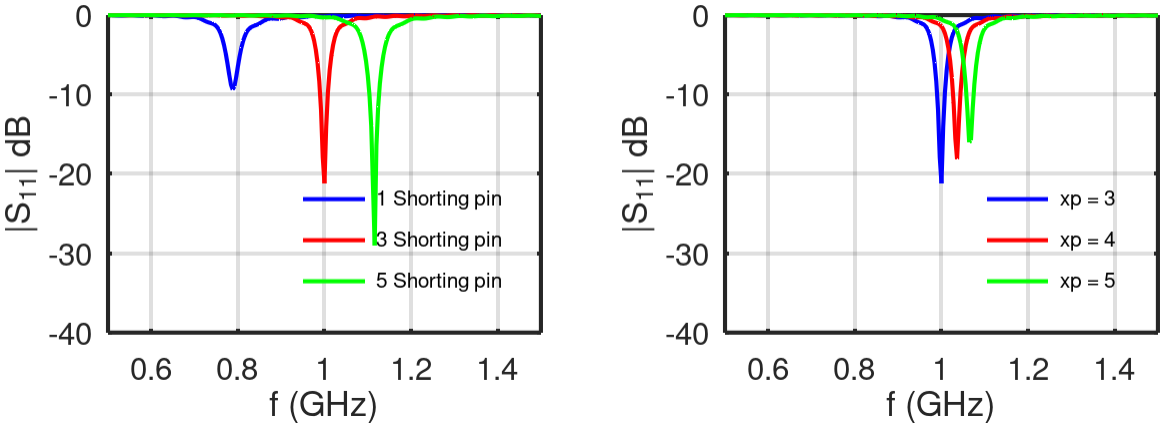

(a) Effect of quantity of shorting pins (b) Effect of variable xp

Figure 4.28: Parametric study of shorting pins

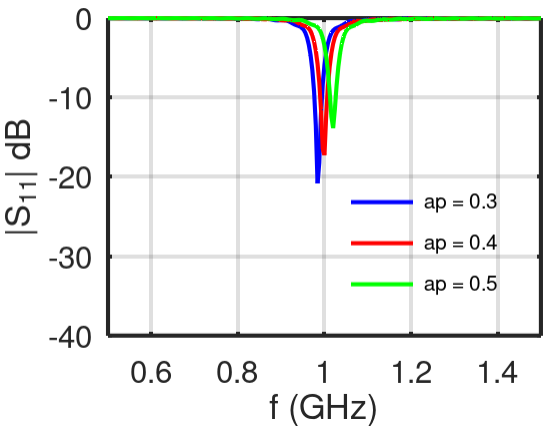

(a) Effect of variable ap

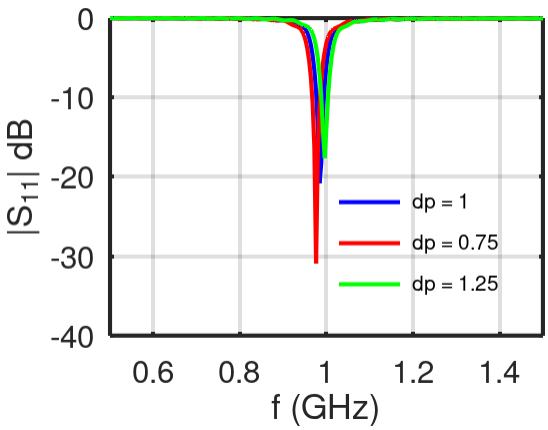

(b) Effect of variable dp

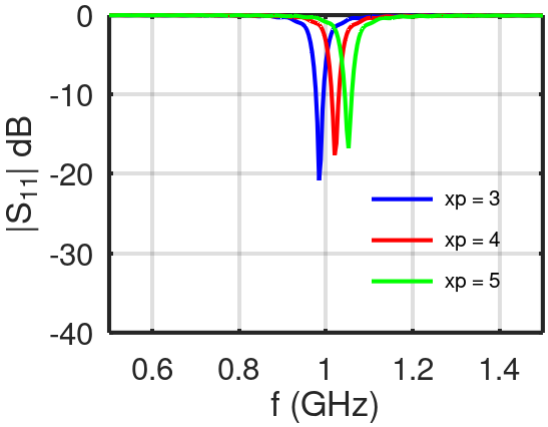

(c) Effect of variable xp

Figure 4.29: Parametric study of shorting pins with superstrate

Table 4.12: Antenna dimensions in order to be resonant at 2.45 GHz with shorting pins with superstrate

Variable	*Dimension (mm)*	*Variable*	*Dimension (mm)*
Lg	20	ap	0.3
Wg	20	dp	0.75
Lp	10.8	xp	3
Wp	16	hsuper	1.6
df	6.6	h	1.6
xf	0		

Following this studies the antenna will be place inside the phantom. With dimensions of table 4.12 we can optimize the antenna to 2.45 GHz ISM frequency band. Simulated results are shown in figure 4.30. This antenna has 316 MHz of bandwidth.

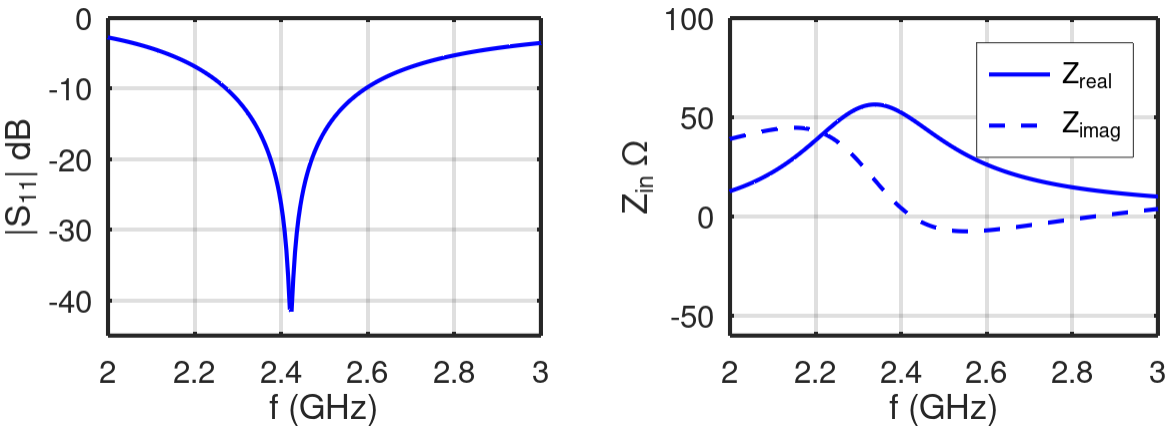

(a) Matching level (b) Impedance

Figure 4.30: Matching level and impedance for antenna with three shorting pins inside the phantom

4.4 Compacted antenna inside phantom

With the miniaturization techniques studied in the previous sections a new antenna can be designed in order to work inside the human body while also being small enough to not cause discomfort. The techniques used to design this antenna will be:

1. Slits in patch;
2. Shorting pins;
3. High permittivity material.

The material used in substrate is Rogers RO3010($\varepsilon_r = 11.2$) and in the superstrate Rogers RT5880($\varepsilon_r = 2.2$). Antenna geometry is shown in figure 4.31 while antenna dimensions are shown in table 4.13. The antenna was placed inside the phantom and the simulated results are shown in figure 4.32.

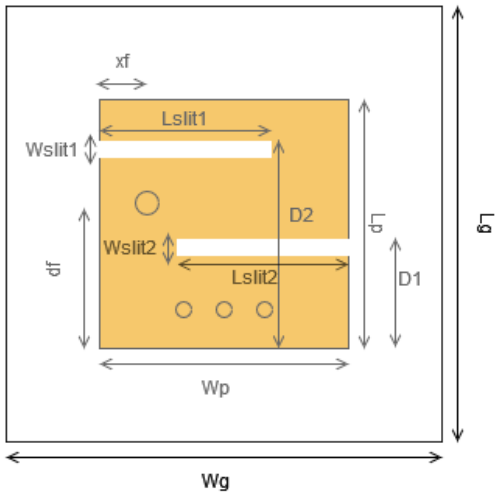

(a) Front view

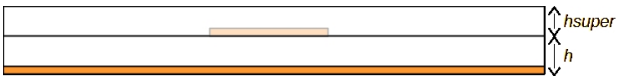

(b) Side view

Figure 4.31: Geometry of in-body antenna designed in this thesis

Table 4.13: Compact antenna dimensions inside the phantom

Variable	*Dimension (mm)*	*Variable*	*Dimension (mm)*
Lg	8.5	Lslit1	5
Wg	8.5	Lslit2	4.5
Lp	6.4	Wslit1	0.5
Wp	7	Wslit2	0.5
d1	2	d2	4
df	3.4	h	1.6
xf	2	hsuper	1.6

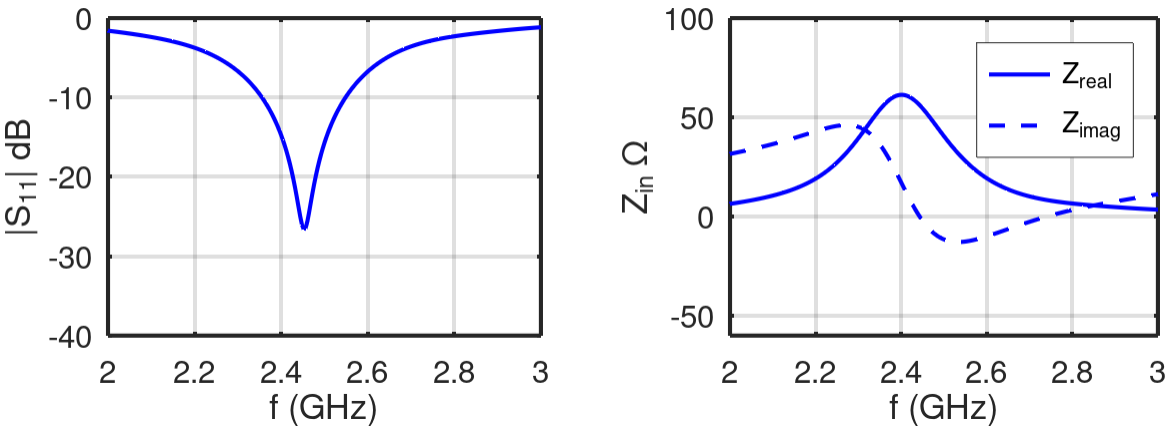

(a) Matching level (b) Impedance

Figure 4.32: Matching level and impedance for compact antenna dimensions from table 4.13

This antenna is tuned to the ISM 2.45 GHz frequency band and is also very compact, with dimensions of 8.5 mm by 8.5 mm by 3.2 mm. This is a very significant reduction in dimensions comparing to the antenna designed in chapter 3 (60 x 60 x 3.2 mm). This antenna also has a bandwidth of 192 MHz, covering the whole frequency band. The materials used in the simulations are not available to use, so a couple of changes will be made to this antenna in order to make it possible to manufacture:

1. The use of a standard SMA connector;

2. The use of the same material as substrate and superstrate.

These changes will make the antenna larger, but it will be possible to manufacture it with the materials available. There is also the need to fix the superstrate, in order to do this, two antennas will be designed; one will hold the superstrate with glue, the other will hold the superstrate with screws. The in-body glue antenna will be smaller but the dielectric properties of the glue may impact antenna performance while the antenna with screws will be larger but the screws are not expected to impact antenna performance.

The in-body glue antenna dimensions are shown in table 4.14 with simulated results being shown in figure 4.33. The simulation was done without adding glue to the in-body antenna however, since it is not expected to impact simulation results.

Table 4.14: Dimensions of the in-body glue antenna

Variable	*Dimension (mm)*	*Variable*	*Dimension (mm)*
Lg	13	df	4.3
Wg	13	h	1.6
Lp	9.7	hsuper	1.6
Wp	9.5	xp	3
D1	6.5	ap	0.35
D2	2.5	dp	0.75
Lslit1	8.1	Wslit	1
Lslit2	7.1	xf	3

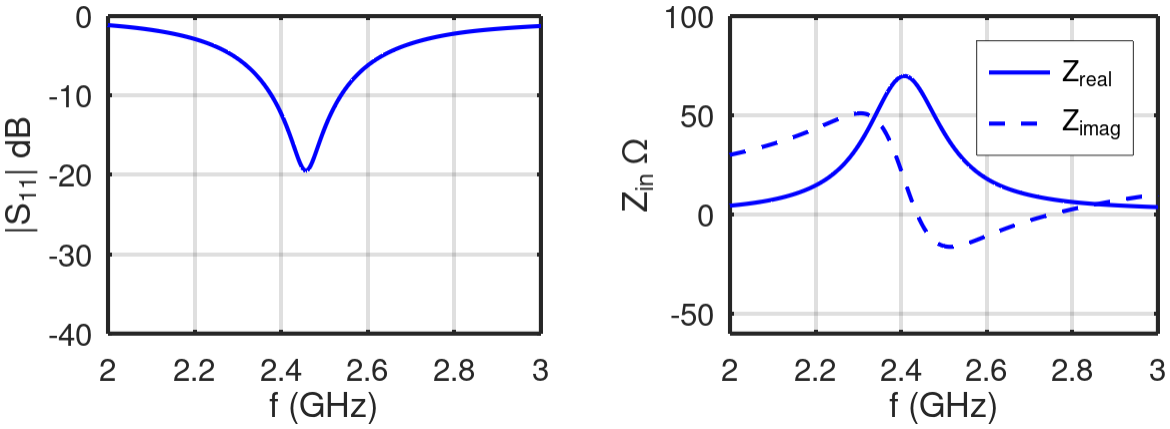

(a) Matching level

(b) Impedance

Figure 4.33: Matching level and impedance for in-body glue antenna with dimensions of table 4.14

The screw antenna needs to be slightly bigger in order to hold the screws. The antenna geometry is shown in figure 4.34 while dimensions are shown in table 4.15. Simulated result is shown in figure 4.35.

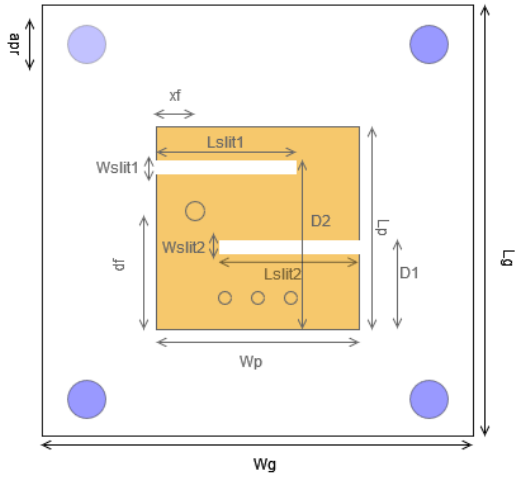

(a) Front view

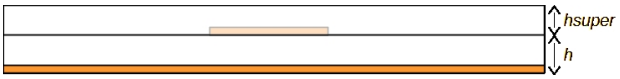

(b) Side view

Figure 4.34: Geometry of in-body antenna designed in this thesis

Table 4.15: Dimensions of the in-body screws antenna

Variable	*Dimension (mm)*	*Variable*	*Dimension (mm)*
Lg	19	df	4.3
Wg	19	h	1.6
Lp	9.7	hsuper	1.6
Wp	9.5	xp	3
D1	2.5	ap	0.35
D2	6.5	dp	0.75
Lslit1	8.1	Wslit	1
Lslit2	7.1	xf	3
apr	1.5		

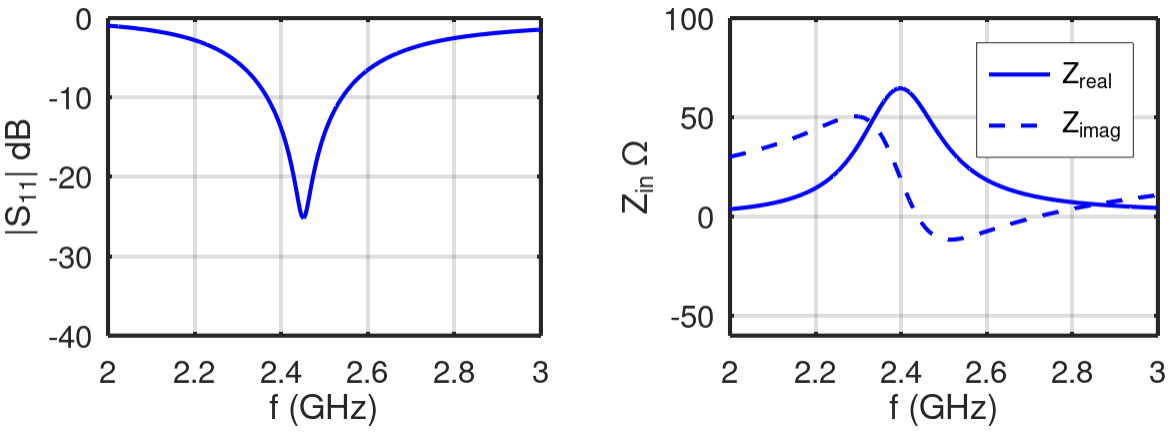

(a) Matching level (b) Impedance

Figure 4.35: Matching level and impedance for in-body glue antenna with dimensions of table 4.15

Both antennas cover the whole ISM 2.45 GHz frequency band and display good results. Both antennas are well matched at 2.45 GHz with bandwidth of 158 MHz and 172 MHz for the the in-body glue and antenna with screws, respectively.

5

Transmission between antennas

In this chapter transmission between antennas will be studied. Both in-body antennas designed in the previous section will communicate with an exterior on-body antenna designed in my bachelors final project. A study on transmission values will be done depending on the depth of the in-body antenna. SAR values will also be calculated for every antenna. Finally, a study characterizing the link-budget will be presented.

5.1 On-body antenna

As said before, this on-body antenna was designed in my bachelors final project but was manufactured and tested during this thesis. An aperture coupled microstrip antenna (figure 5.1) was designed due to its various parameters that could be changed to tune the antenna performance. Unlike in the case of in-body antennas, where size constraints are critical, miniaturization techniques were not employed in designing the on-body antenna.

The antenna measures 58 x 45 x 3.2 mm. Antenna full dimensions are in table 5.1. The chosen material for this antenna was FR-4, which has a dielectric constant of ε_r = 4.3 and loss tangent δ = 0.025 at 2.45 GHz. The input match obtained by simulation are shown in figure 5.2. The antenna is well matched at 2.45 GHz with bandwidth of 1 GHz.

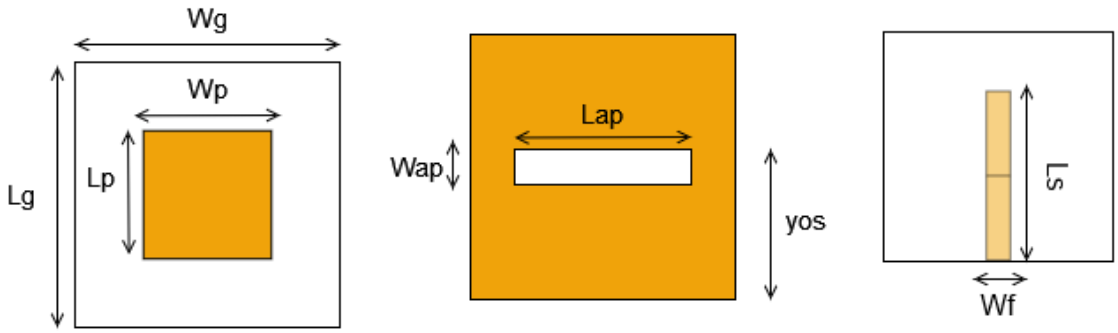

(a) Front view (b) Middle view (b) Back view

Figure 5.1: Aperture coupled patch antenna

Table 5.1: Dimensions of on-body antenna

On-body antenna			
Variable	*Dimension (mm)*	*Variable*	*Dimension (mm)*
Lg	45	Ls	31.5
Wg	58	hsubA	1.6
Lp	22.5	hsubB	1.6
Wp	29	yos	17.5
Lap	21.5	Wap	5
Wf	3		

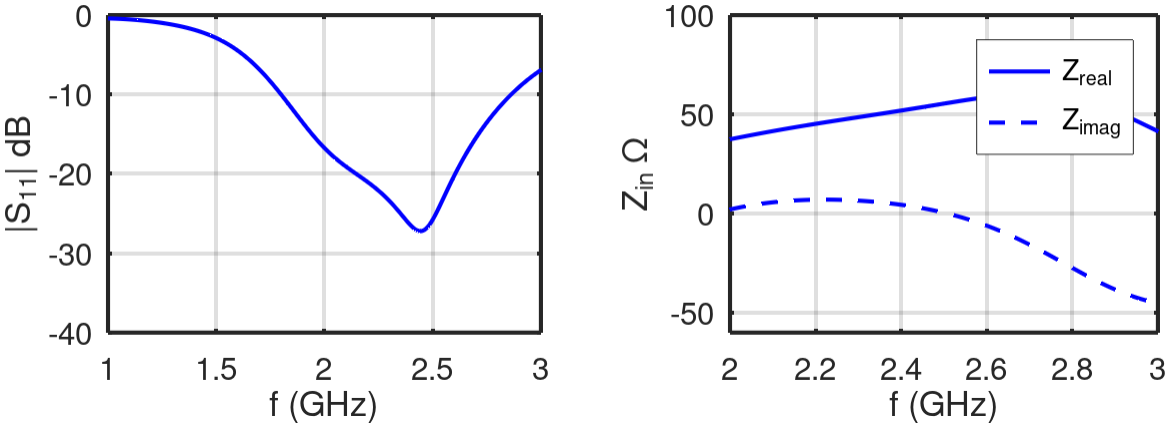

(a) Matching level (b) Impedance

Figure 5.2: Matching level and impedance for antenna with dimensions of table 5.1

Table 5.2: Phantom dimensions

Wc [mm]	*Lc [mm]*	*Hc [mm]*
200	*400*	*150*

5.2 Transmission

Antennas will be placed as illustrated in figure 5.3. The phantom for this section will be bigger, in order to get the more accurate transmission results. Phantom dimensions for this section are shown in table 5.2.

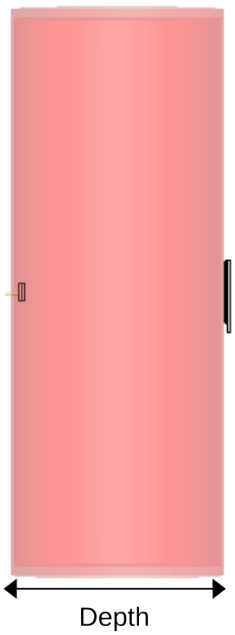

Figure 5.3: Transmission between antennas

Simulated results for both in-body antennas are shown in figures 5.4. Both antennas display a -75 dB transmission value when placed at the opposite edge of the phantom.

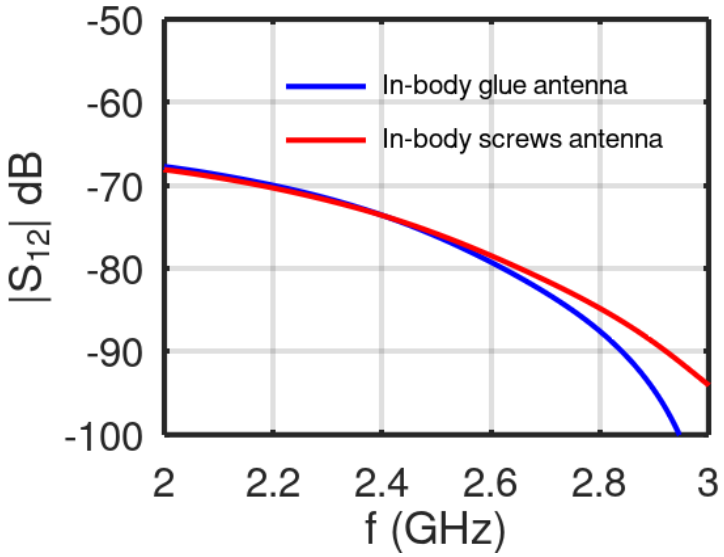

Figure 5.4: S_{12} for both in-body antennas

A parametric study of the depth variable was done. In figure 5.5 simulated results are shown, for the in-body glue antenna and the in-body screw antenna respectively.

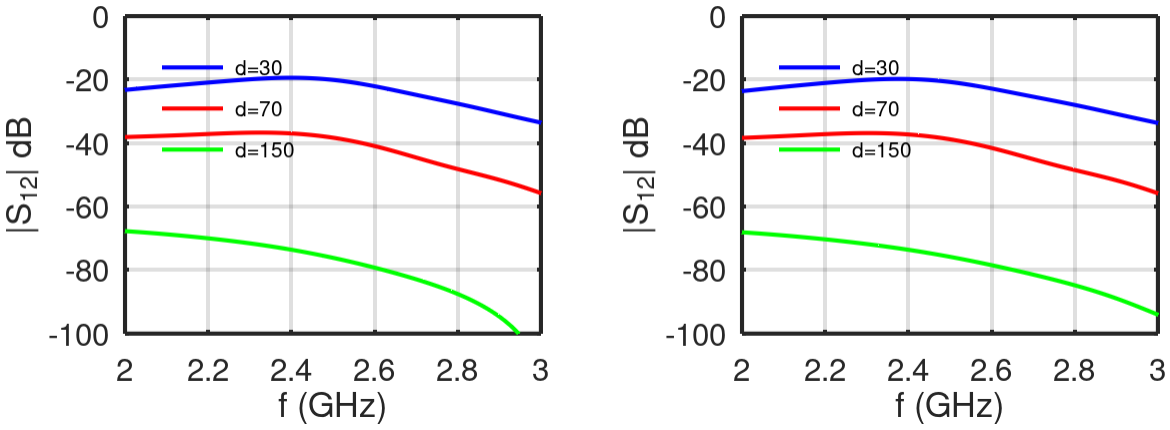

(a) In-body glue antenna

(b) In-body screws antenna

Figure 5.5: Parametric study of depth of the antenna (dimensions in mm)

The shorter the distance between in-body antennas and the on-body antenna, the better S_{12} we can achieve. Transmission values with the antenna at the center of the phantom are around -40 dB for both antennas, an improvement of 35 dB when compared to the antennas placed at opposing edges.

5.3 SAR values

In this section SAR values will be studied. The radiation absorbed by the human body from electromagnetic devices may be a health hazard and SAR legislation imposes an average SAR of 1.6 W/kg when the averaging volume is 1 g or 2 W/kg when the averaging volume is 10 g. For this study both antennas were supplied with an input power of 0.5 W (default value for calculating SAR in CST) and a mass density of 1000 Kg/m3 was used in the phantom. Under these conditions SAR values and maximum allowed input power for all antennas are shown in table 5.3. The maximum allowed input power that we can use to comply with SAR legislation is 9.2 mW for the in-body glue antenna, 9.6 mW for the in-body screw antenna and 31.7 mW for the on-body antenna.

Table 5.3: SAR values and maximum allowed input power to comply with SAR legislation for each antenna

Antenna	Averaging Volume(g)	Maximum allowed input power(mW)	SAR Values for 0.5W(W/Kg)
Glue antenna	1	9.2	86.19
	10	34.4	29
Screw antenna	1	9.6	82.58
	10	38	26.15
On-body antenna	1	31.7	25
	10	67.6	14.68

The values for the maximum allowed input power for the in-body antennas are much higher than the allowed input power for in-body devices (25 μW) [31], which means the antennas are safe to use from a SAR point of view.

The values for the maximum allowed input power for the on-body antenna is also much higher than the allowed input power for on-body devices (10 mW).

5.4 Link budget calculation

There must be a robust connection between both antennas in order for this system to have connectivity. The availability of the communication is decided by C/N_0 (Signal to noise ratio). If the link C/N_0 exceeds the required C/N_0, wireless communication is possible [31]. With the use of equation (5.1) we can calculate the link C/N_0 for this system and with equation 5.2 we can calculate the required value of C/N_0 for successful transmission. These equations were taken from [31].

$$C1/N_0 = Pt + Gt - L + Gr - N_0[dB/Hz] \tag{5.1}$$

$$C1/N_0 = E_b/N_0 + 10log_{10}(B_r) \tag{5.2}$$

Where:

- Pt is transmitted power in dBW;
- Gt and Gr are transmitted and receiver antenna gain in dBi, respectively;
- Lf is free space loss in dB;
- N_0 is noise power density in dB/Hz;
- E_b/N_0 in dB;
- Br is bit rate.

In this particular system we can replace both gains (Gr and Gt) and the attenuation (L) with the already calculated S_{12} parameter taken from CST. The antennas were positioned 150 mm apart inside the phantom which results in a S_{12} value of -74.78 dB and -74.64 dB for the in-body glue antenna and the in-body screws antenna, respectively. Transmitted power (Pt) and noise power density (N_0) values are 25 μW (maximum input power allowed for in-body devices) and -202.17 dB/Hz (noise power density at room temperature), respectively. This results in C/N_0 of 81.39 and 81.53 for the in-body glue antenna and the in-body screws antenna. Equaling both equations we can get:

$$B_r = 10^{\frac{C/N_0 - E_b/N_0}{10}} \tag{5.3}$$

Throughput depends on Bit error rate (BER) and modulation used. For this system BPSK modulation and three different BER values (presented in table 5.4) will be used in order to calculate the maximum throughput possible. Results are present in figure 5.6.

Table 5.4: E_b/N_0 values for different BER's for BPSK modulation

BER	E_b/N_0
10^{-4}	*8.38*
10^{-5}	*9.58*
10^{-6}	*10.51*

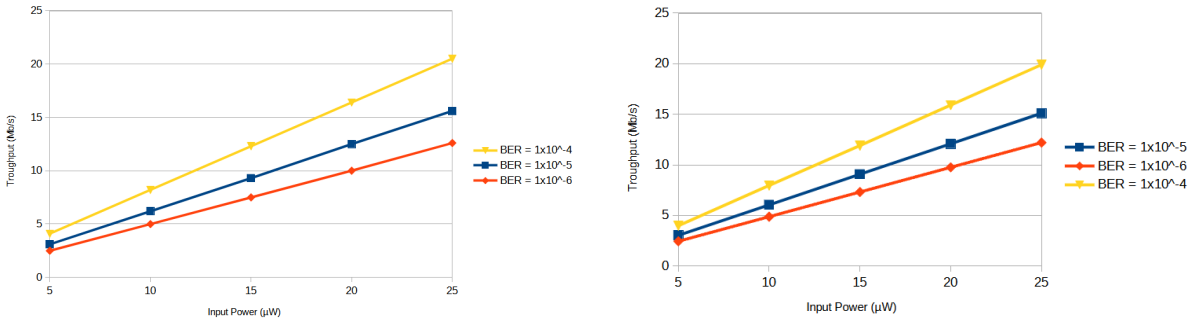

(a) In-body screw antenna (b) In-body glue antenna

Figure 5.6: Throughput for both in-body antennas spaced 150 mm

With this configuration, maximum possible throughput is 19.99 Mb/s and 20.65 Mb/s with BER of 10^{-4} for the in-body glue antenna and the in-body screw antenna, respectively. As expected, throughput decreases with the decrease of BER, with the system only achieving 12 Mb/s with a BER of 10^{-6}.

When the antennas are positioned 70mm apart from each other the results improve significantly. As shown in figure 5.7, throughput for the in-body glue antenna and the in-body screw antenna reaches 107 Gb/s and 97 Gb/s, respectively.

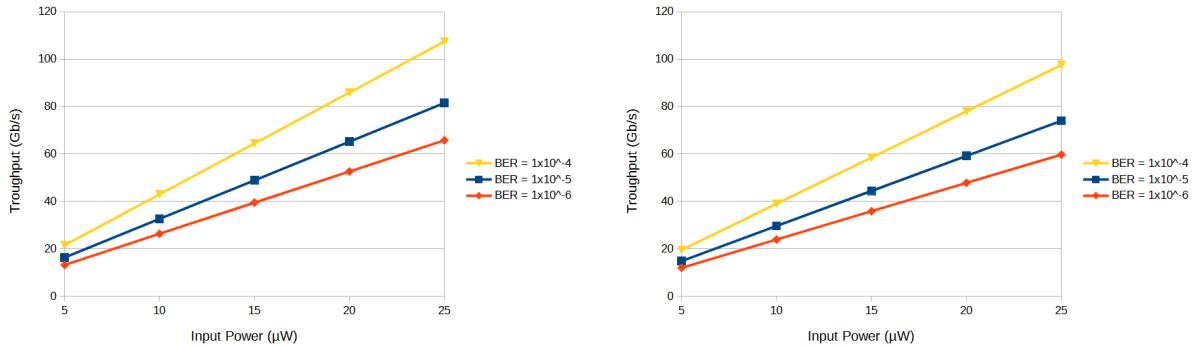

(a) In-body screw antenna (b) In-body glue antenna

Figure 5.7: Throughput for both in-body antennas spaced 70 mm

6

Experimental results

Both in-body antennas mentioned in the previous chapters were built. Both antennas will be tested using pork tissue. The on-body antenna that was designed in my bachelor's degree was also built during this thesis in order to validate simulated results. This chapter will be divided in four sections. The first section will talk about the setup used to measure the antennas, the second and third sections will be about the in-body glue and in-body screw antennas, respectively. The last section will be about the on-body antenna.

6.1 Setup

To test the antennas a pork meat piece was bought. This piece had dimensions of 18 cm by 13 cm by 5 cm and is shown in figure 6.1. The pork piece was cut and wrapped in plastic in order to place the antennas inside as shown in figure 6.2. Measurements were done with a Vector Network Analyzer (VNA) and processed using Octave.

(a) Length of pork piece

(b) Width of pork piece

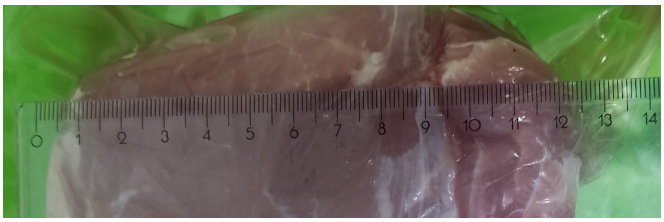

(b) Thickness of pork piece

Figure 6.1: Fabricated in-body antenna

Figure 6.2: Pork piece cut and wrapped in plastic

6.2 In-body glue antenna

Images of the manufactured in-body glue antenna are shown in figure 6.3. The antenna was placed inside of pork tissue for testing as shown in figure 6.4. Measurement results are shown in figure 6.5 and show that when the antenna is pressed hard against the pork piece, a good agreement between simulations and measurements is achieved and the antenna covers the whole ISM 2.45 GHz frequency band. However, when it is lightly pressed, the antenna frequency is detuned.

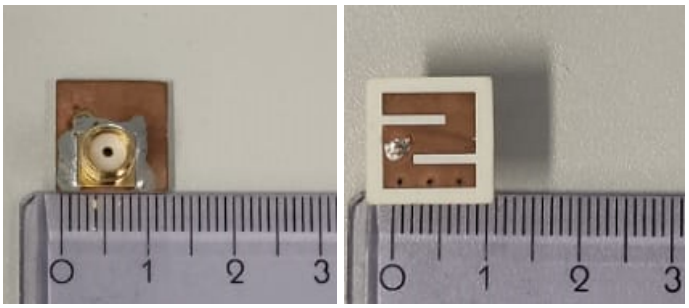

(a) Back view (b) Front view

Figure 6.3: Fabricated in-body antenna

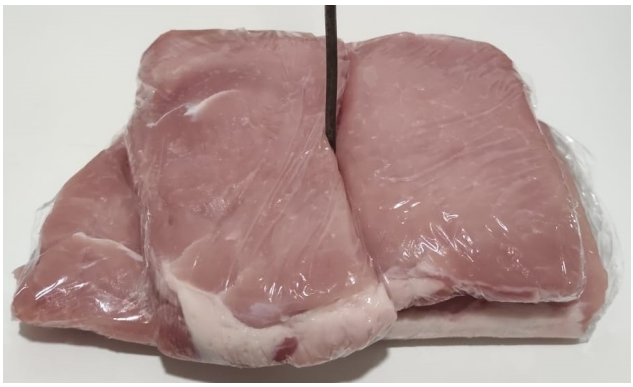

Figure 6.4: In-body antenna placed in pork tissue

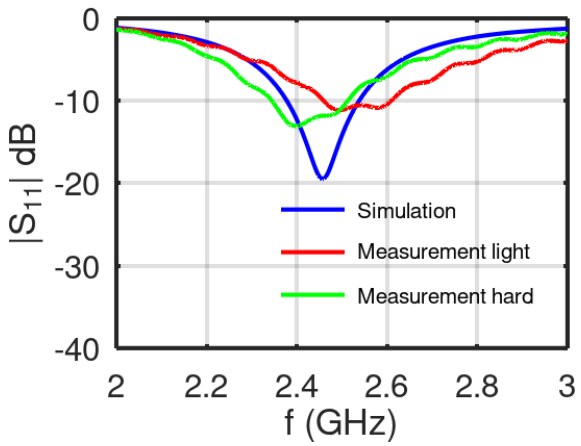

Figure 6.5: In-body glue antenna simulation and measurement results

6.3 In-body screws antenna

The manufactured in-body screws antenna is shown in figure 6.6. The testing scenario is also similar to the previous antenna. In figure 6.7 simulated and measurement results are shown and results are similar to the previous antenna, when it is pressed hard against the pork piece, the antenna is close to the simulated results. However, when it is lightly pressed, frequency is detuned.

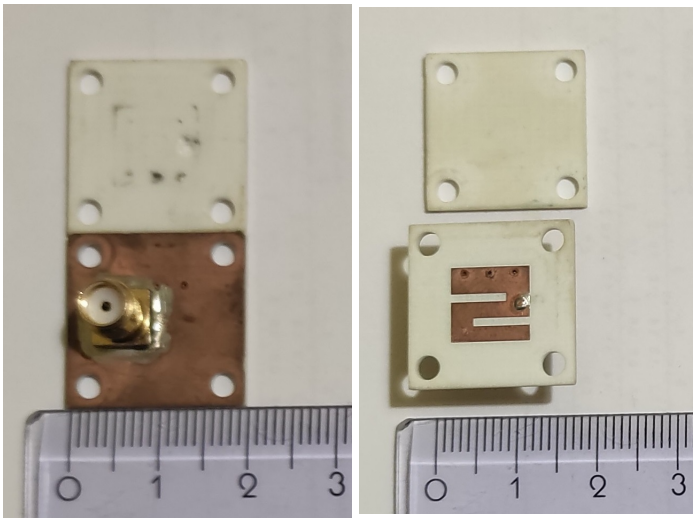

(a) Back view (b) Front view

Figure 6.6: Fabricated in-body screws antenna

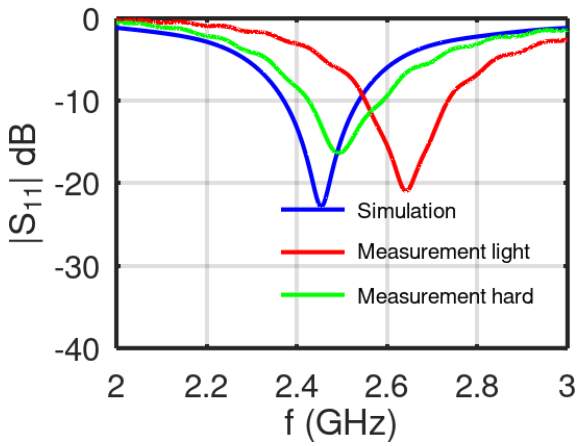

Figure 6.7: In-body screw antenna simulation and measurement results

6.4 On body antenna

In this section the results of the on-body antenna will be shown. The fabricated antenna is shown in figure 6.8.

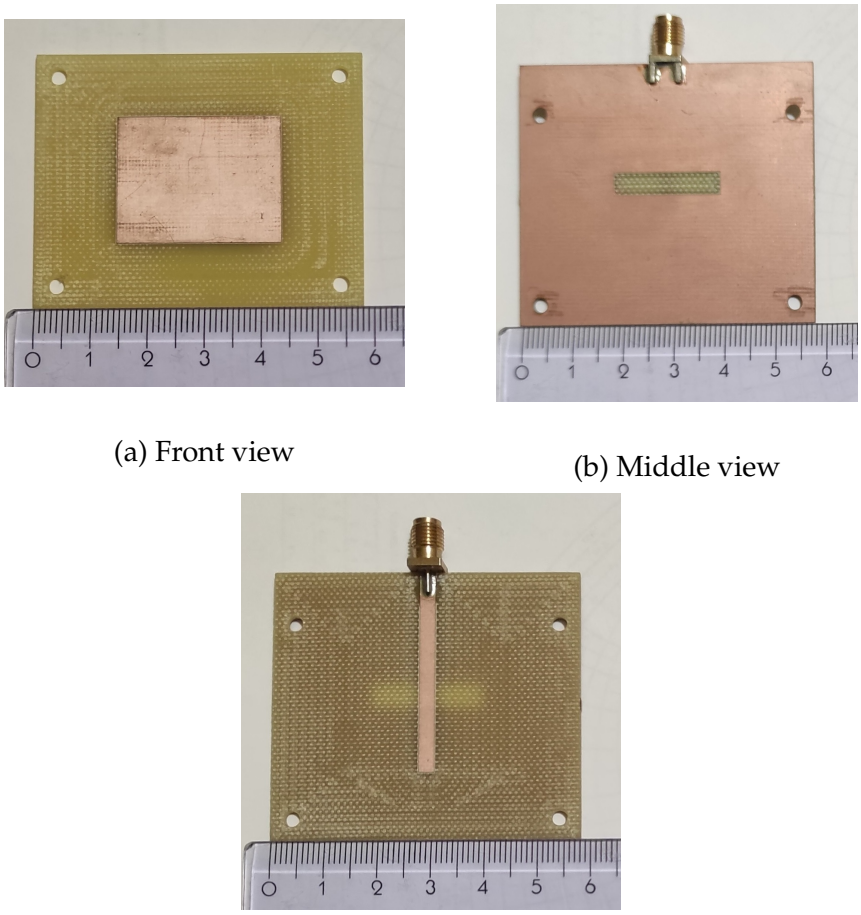

(a) Front view

(b) Middle view

(b) Back view

Figure 6.8: Fabricated on-body antenna

The testing scenario is shown in figure 6.9. As in the design, in the measurements the antenna is not in contact with the pork tissue, with a layer of 2mm of styrofoam separating the two.

Simulation and measurement results are shown in figure 6.10. Although the antenna covers the whole ISM 2.45 GHz ISM frequency band, performance was worse than expected likely due to the use of FR-4 as substrate material.

S_{12} measurements were not taken because, to achieve accurate results, the piece of pork needed to match the dimensions of table 5.2.

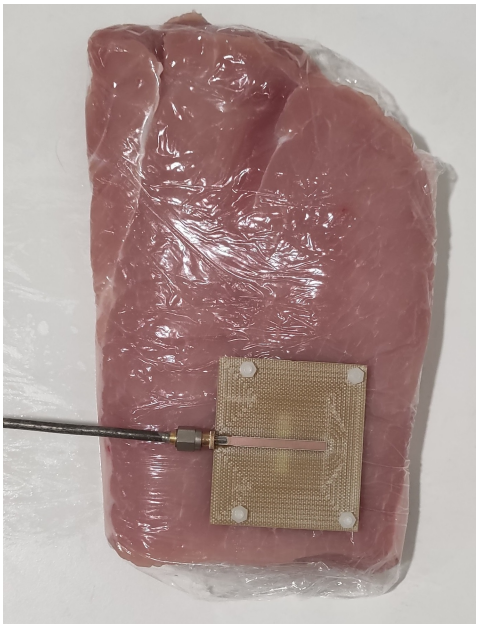

Figure 6.9: On-body antenna testing scenario

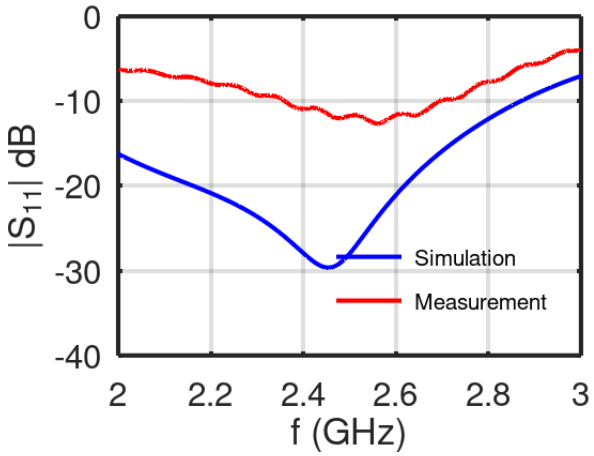

Figure 6.10: On-body antenna simulation and measurement results

7

Conclusion and future work

This chapter will focus on conclusions for this thesis and possible future work.

7.1 Conclusion

This dissertation had the main objective of designing a small antenna capable of working inside the human body. A state of art for in-body antennas was presented. Antennas for this type of applications need to be compact in size and biocompatible in order to not cause problems to the patients. At higher frequencies, attenuation through the biological tissues increases dramatically as the frequency increases. For example, at frequencies between 3 and 5 GHz attenuation is as high as 20-30 dB for every 2 cm of biological tissue [3].

This attenuation caused by the human body can be reduced with the help of a superstrate. In this thesis we find that the lower the value of ε_r, the better adaptation we can achieve. The use of a superstrate however, proved to be a problem in the fabrication of the antenna.

A microstrip patch antenna is suggested for in-body use. However, because the antenna is too big, miniaturization techniques are studied in order to compact the antenna size. A second patch antenna was suggested. This antenna has dimensions of 8.5 x 8.5 x 3.2 mm and has a good performance, covering the whole ISM 2.45 GHz frequency band.

However, this antenna is too small to cheaply fabricate. The connector needed in order to feed an antenna like this will be expensive, and it was not in the scope of this thesis.

Because of this, two other antennas were designed; one with dimensions of 13 x 13 x 3.2 mm and the other with 19 x 19 x 3.2 mm. Glue was used in order to hold the superstrate in the smaller antenna, while screws were used to hold the superstrate in the bigger antenna. These antennas displayed good results and covered the whole ISM 2.45 GHz frequency band.

Transmission between antennas showed positive results with a transmission coefficient of -75 dB at 2.45 GHz. SAR and maximum allowed input power values were calculated. Additionally, transmission between antennas improved significantly when the in-body antenna was positioned at the center of the phantom, with a transmission value of -40 dB.

In the case of the in-body antennas, measured results were similar to the simulated when the antennas were pressed against the pork meat. The on-body antenna measured results were worse than the simulated ones, likely due to the use of FR-4 as substrate material.

Link budget between antennas was also studied. When the antenna was placed 70 mm deep in the phantom, throughput values reached 97 and 107 Gb/s for the in-body glue antenna and the in-body screws antenna, respectively.

7.2 Future Work

In future research, several important areas warrant exploration:

- Multi-Layered Phantom Study: Future work should focus on the study of multi-layered phantoms that can closely resemble the complexity of the human body and provide more accurate results;
- Bio-compatible materials: The inclusion of bio-compatible materials as shown to improve radiation efficiency and SAR values in prior research, and deserves a comprehensive investigation within the context of this antenna system. The bio-compatible materials are also needed so the antenna is not in touch with the human tissue;
- Experimental Validation: Although experimental results were presented in this thesis, the link-budget results need validation as well;

- Redesigning the on-body antenna: The on-body antenna used in this thesis was designed in a bachelors project. The experimental results of the antenna were not as good as anticipated. The use of FR-4 likely contributed to this. A redesign of the antenna may provide better results;
- Flexible materials: The in-body antenna is a planar microstrip antenna, which means that it only communicates in one direction. Bending may be possible with the use of flexibles materials to fabricate the antenna and the radiation pattern may be more omnidirectional and allow for more healthcare applications.

By investigating these areas in future research, a more comprehensive understanding of in-body and on-body antenna systems can be attained, ultimately contributing to advancements in medical and wearable communication technologies.

References

[1] Gurveer Kaur, Amandeep Kaur, Gurpreet Kaur Toor, Balwinder S. Dhaliwal, and Shyam Sundar Pattnaik, "Antennas for biomedical applications", *Biomedical Engineering Letters*, vol. 5, no. 3, pages 203–212, Sep. 1, 2015, ISSN: 2093-985X. DOI: 10.1007/s13534-015-0193-z.

[2] Hari Singh, Binod Kumar Kanaujia, Sachin Kumar, and Kunal Srivastava, "A compact wideband flexible antenna for wireless medical telemetry services", *Wireless Personal Communications*, vol. 123, no. 3, pages 2393–2411, Apr. 1, 2022, ISSN: 1572-834X. DOI: 10.1007/s11277-021-09246-w.

[3] Asimina Kiourti and Konstantina S. Nikita, "A review of in-body biotelemetry devices: Implantables, ingestibles, and injectables", *IEEE Transactions on Biomedical Engineering*, vol. 64, no. 7, pages 1422–1430, Jul. 2017, ISSN: 1558-2531. DOI: 10.1109/TBME.2017.2668612.

[4] Yongxin Guo and Hui Chu, "Antenna-in-package design for wireless ingestible capsule", in *2017 International Workshop on Electromagnetics: Applications and Student Innovation Competition*, May 2017, pages 56–57. DOI: 10.1109/iWEM.2017.7968765.

[5] Carlos Alberto Barreiro Mendes, "A wearable dual-mode printed antenna for body-centric applications", Ph.D. dissertation, 2017.

[6] Eric Y. Chow, Milton M. Morris, and Pedro P. Irazoqui, "Implantable RF medical devices: The benefits of high-speed communication and much greater communication distances in biomedical applications", *IEEE Microwave Magazine*, vol. 14, no. 4, pages 64–73, Jun. 2013, ISSN: 1557-9581. DOI: 10.1109/MMM.2013.2248586.

[7] Asimina Kiourti and Konstantina S. Nikita, "A review of implantable patch antennas for biomedical telemetry: Challenges and solutions [wireless corner]", *IEEE Antennas and Propagation Magazine*, vol. 54, no. 3, pages 210–228, Jun. 2012, ISSN: 1558-4143. DOI: 10.1109/MAP.2012.6293992.

[8] Markus Grimm and Dirk Manteuffel, "Antennas and propagation for on-, off- in-body communications", in *Ultra-Wideband Radio Technologies for Communications, Localization and Sensor Applications*, Reiner Thom, Ed., InTech, Mar. 13, 2013, ISBN: 978-953-51-0936-5. DOI: 10.5772/55080. (visited on 11/04/2022).

[9] Konstantinos A. Psathas, Asimina Kiourti, and Konstantina S. Nikita, "Biocompatibility of implantable antennas: Design and performance considerations", in *The 8th European Conference on Antennas and Propagation (EuCAP 2014)*, ISSN: 2164-3342, Apr. 2014, pages 1566–1570. DOI: 10.1109/EuCAP.2014.6902083.

[10] Francesco Merli, Benjamin Fuchs, Juan R. Mosig, and Anja K. Skrivervik, "The effect of insulating layers on the performance of implanted antennas", *IEEE Transactions on Antennas and Propagation*, vol. 59, no. 1, pages 21–31, Jan. 2011, ISSN: 1558-2221. DOI: 10.1109/TAP.2010.2090465.

[11] Fu-Jhuan Huang, Chien-Ming Lee, Chia-Lin Chang, Liang-Kai Chen, Tzong-Chee Yo, and Ching-Hsing Luo, "Rectenna application of miniaturized implantable antenna design for triple-band biotelemetry communication", *IEEE Transactions on Antennas and Propagation*, vol. 59, no. 7, pages 2646–2653, Jul. 2011, ISSN: 1558-2221. DOI: 10.1109/TAP.2011.2152317.

[12] Ashok Kumar Srinivasan and T. Shanmuganantham, "Design of implantable CPW fed monopole antenna for ISM band applications", *AEU - International Journal of Electronics and Communications*, vol. 68, pages 661–666, Jul. 1, 2014. DOI: 10.1016/j.aeue.2014.02.010.

[13] Hans Permana, Qiang Fang, and Irena Cosic, "3-layer implantable microstrip antenna optimised for retinal prosthesis system in MICS band", in *International Symposium on Bioelectronics and Bioinformations 2011*, Nov. 2011, pages 65–68. DOI: 10.1109/ISBB.2011.6107646.

[14] Farhad Gozasht and Ananda Sanagavarapu Mohan, "Miniaturized slot PIFA antenna for tripleband implantable biomedical applications", in *2013 IEEE MTT-S International Microwave Workshop Series on RF and Wireless Technologies for Biomedical and Healthcare Applications (IMWS-BIO)*, Dec. 2013, pages 1–3. DOI: 10.1109/IMWS-BIO.2013.6756180.

[15] Sarosh Ahmad, Bilal Manzoor, Kashif Paracha, Sajjad Haider, Maryam Liaqat, Ahmed Al-Gburi, Adnan Ghaffar, Mohammad Alibakhshikenari, and Mariana Dalarsson, "A wideband bear-shaped compact size implantable antenna for in-body communications", *Applied Sciences*, vol. 12, page 2859, Mar. 10, 2022. DOI: 10.3390/app12062859.

[16] Chien-Ming Lee, Tzong-Chee Yo, and Ching-Hsing Luo, "Compact broadband stacked implantable antenna for biotelemetry with medical devices", in *2006 IEEE Annual Wireless and Microwave Technology Conference*, Dec. 2006, pages 1–4. DOI: 10.1109/WAMICON.2006.351945.

[17] J. Ha, K. Kwon, and J. Choi, "Compact zeroth-order resonance antenna for implantable biomedical service applications", *Electronics Letters*, vol. 47, no. 23, pages 1267–1269, Nov. 10, 2011, Publisher: IET Digital Library, ISSN: 1350-911X. DOI: 10.1049/el.2011.2999.

[18] Al-Hasan Mu'ath, Penchala Reddy Sura, Amjad Iqbal, Ismail Ben Mabrouk, and Jun-Jiat Tiang, "Low-profile dual-band implantable antenna for compact implantable biomedical devices", *AEU - International Journal of Electronics and Communications*, vol. 138, page 153 896, Aug. 1, 2021, Publisher: Urban & Fischer, ISSN: 1434-8411. DOI: 10.1016/j.aeue.2021.153896.

[19] Yang Feng, Zhaonan Li, Lin Qi, Wanting Shen, and Gaosheng Li, "A compact and miniaturized implantable antenna for ISM band in wireless cardiac pacemaker system", *Scientific Reports*, vol. 12, no. 1, page 238, Jan. 7, 2022, Publisher: Nature Publishing Group, ISSN: 2045-2322. DOI: 10.1038/s41598-021-04404-3. [Online]. Available: https://www.nature.com/articles/s41598-021-04404-3 (visited on 04/09/2024).

[20] Sang il Kwak, K. Chang, and Y.J. Yoon, "Small spiral antenna for wideband capsule endoscope", *Electronics Letters*, vol. 42, pages 1328–1329, Feb. 1, 2006. DOI: 10.1049/el:20062074.

[21] Sang Il Kwak, Kihun Chang, and Young Joong Yoon, "The helical antenna for the capsule endoscope", in *2005 IEEE Antennas and Propagation Society International Symposium*, ISSN: 1947-1491, vol. 2B, Jul. 2005, 804–807 vol. 2B. DOI: 10.1109/APS.2005.1552139.

[22] Ke Zhang, Changrong Liu, Xueguan Liu, Honglong Cao, Yudi Zhang, Xinmi Yang, and Huiping Guo, "A conformal differentially fed antenna for ingestible capsule system", *IEEE Transactions on Antennas and Propagation*, vol. 66, no. 4, pages 1695–1703, Apr. 2018, ISSN: 1558-2221. DOI: 10.1109/TAP.2018.2804673.

[23] Md Shamsul Arefin, Jean-Michel Redoute, and Mehmet Rasit Yuce, "Meandered conformai antenna for ISM-band ingestible capsule communication systems", in *2016 38th Annual International Conference of the IEEE Engineering in Medicine and Biology Society (EMBC)*, ISSN: 1558-4615, Aug. 2016, pages 3031–3034. DOI: 10.1109/EMBC.2016.7591368.

[24] Wonbum Seo, Uisheon Kim, Soonyong Lee, Kyeol Kwon, and Jaehoon Choi, "A meandered inverted-f capsule antenna for an ingestible medical communication system", *Microwave and Optical Technology Letters*, vol. 54, no. 7, pages 1761–1765, 2012, _eprint: https://onlinelibrary.wiley.com/doi/pdf/10.1002/mop.26869, ISSN: 1098-2760. DOI: 10.1002/mop.26869. [Online]. Available: https://onlinelibrary.wiley.com/doi/abs/10.1002/mop.26869 (visited on 03/08/2023).

[25] Denys Nikolayev, Maxim Zhadobov, Laurent Le Coq, Pavel Karban, and Ronan Sauleau, "Robust ultraminiature capsule antenna for ingestible and implantable applications", *IEEE Transactions on Antennas and Propagation*, vol. 65, no. 11, pages 6107–6119, Nov. 2017, ISSN: 1558-2221. DOI: 10.1109/TAP.2017.2755764. [Online]. Available: https://ieeexplore.ieee.org/document/8048539 (visited on 05/09/2024).

[26] Michael J. Christoe, Natthaporn Phaoseree, Jialuo Han, Aron Michael, Shaghik Atakaramians, and Kourosh Kalantar-Zadeh, "Meandering pattern 433 MHz antennas for ingestible capsules", *IEEE Access*, vol. 9, pages 91 874–91 882, 2021, ISSN: 2169-3536. DOI: 10.1109/ACCESS.2021.3092068. [Online]. Available: https://ieeexplore.ieee.org/abstract/document/9464241 (visited on 05/09/2024).

[27] Constantine A. Balanis. "Antenna theory: Analysis and design, 4th edition | wiley", Wiley.com. (2016), [Online]. Available: https://www.wiley.com/en-us/Antenna+Theory%3A+Analysis+and+Design%2C+4th+Edition-p-9781118642061 (visited on 03/16/2023).

[28] R.Fossi D.Andreuccetti and C.Petrucci, *An internet resource for the calculation of the dielectric properties of body tissues in the frequency range 10 Hz - 100 Ghz*, http://niremf.ifac.cnr.it/tissprop/, 1996.

[29] Denys Nikolayev, Maxim Zhadobov, Pavel Karban, and Ronan Sauleau, "Increasing the radiation efficiency and matching stability of in-body capsule antennas", in *2016 10th European Conference on Antennas and Propagation (EuCAP)*, Apr. 2016, pages 1–5. DOI: 10.1109/EuCAP.2016.7481314.

[30] Kin-Lu Wong. "Compact and broadband microstrip antennas | wiley", Wiley.com. (2002), [Online]. Available: https://www.wiley.com/en-us/Compact+and+Broadband+Microstrip+Antennas-p-9780471465737 (visited on 03/18/2023).

[31] Wei Xia, Kazuyuki Saito, Masaharu Takahashi, and Koichi Ito, "Performances of an implanted cavity slot antenna embedded in the human arm", *IEEE Transactions on Antennas and Propagation*, vol. 57, no. 4, pages 894–899, Apr. 2009, ISSN: 1558-2221. DOI: 10.1109/TAP.2009.2014579. [Online]. Available: https://ieeexplore.ieee.org/document/4812245 (visited on 06/17/2024).